| | |
|---|---|
| Manuscript Number: | IJRMHM-D-21-00512R1 |
| Article Type: | Research Paper |
| Keywords: | WC-FeNiCo hardmetals, DSC, C-window, Phase diagram, Thermodynamic database |
| Corresponding Author: | Tomas Soria-Biurrun, Degree in Chemistry<br>CEIT-BRTA and TECNUN<br>SPAIN |
| First Author: | Tomas Soria-Biurrun, Degree in Chemistry |
| Order of Authors: | Tomas Soria-Biurrun, Degree in Chemistry |
| | Jose M. Sánchez-Moreno, PhD. Physics |
| | Karin Frisk, PhD. Materials Science |
| Abstract: | The liquid phase formation temperatures of the quinary system W-C-Co-Fe-Ni with a ratio of Fe:Co:Ni = 40:20:40 were determined by means of DSC analysis. Besides, the experimental C-window of this system with a binder content of 14.3 ± 2 wt.% is accurately defined. Based on the experimental results, a thermodynamic modelling is carried out using the CALPHAD approach. Temperature-composition sections of the W-C-Co-Fe-Ni system with different binder contents are calculated to verify the rationality of the present modelling. There is a good correlation between the experimental and calculated results showing that the experimental data can be well reproduced by the present modelling. |
| Response to Reviewers: | |

MEMBER OF
BASQUE RESEARCH
& TECHNOLOGY ALLIANCE

July-22th-2021

Dear Editor:

We would like to submit the article entitled "Experimental and theoretical study of WC-40Fe-20Co-40Ni" for publication in the International Journal of Refractory Metals and Hard Materials. Please, do not hesitate to contact us if you have any questions.

Yours sincerely,

Tomas Soria-Biurrun

CEIT-BRTA. Paseo Manuel de Lardizabal, 15, 20018, San Sebastián, Spain.

phone: 34-943-212800
fax:34-943-213076
email: tsoria@ceit.es

**Manuscript Number: IJRMHM-D-21-00512**

**Title: Experimental and theoretical study of WC-40Fe-20Co-40Ni**

**Journal: International Journal of Refractory Metals and Hard Materials**

**Answers to Reviewer # 1 comments:**

The paper presents experimental data of thermal equilibrium for Fe-Co-Ni-W-C alloy and theoretical computation of it based on CALPHAD method, improving data from: P. Zhou, Y. Peng, C. Buchegger, Y. Du, W. Lengauer, Experimental investigation and thermodynamic assessment of the C-Co-Fe-Ni-W system, Int. J. Refract. Met. Hard Mater. 54 (2016) 60-69.

1. **The paper is well prepared (the only improvement is my recommendation to add labels to the equations (1) - (3) and in eq.(1) give "represents" instead of "=" in the description of indexes i,j,k,l, because 4 does not = 5).**

**Answer:** We agree with the reviewer´s comment. We have added labels to the equations (1)-(3). Moreover, we have written in eq. (1) and eq. (3) "represents" instead of "=" in the description of indexes i,j,k,l, and i, j, k respectively. We marked these changes in blue in the revised version.

2. **For possibility to check the calculations, I recommend to add thermodynamic database as Supplementary material to the paper (in that case the Table 2 can be omitted).**

**Answer:** We appreciate the reviewer comment and agree with it. Table 2 has been omitted (changed by Table S1 and marked it in blue in the revised version) and we have added thermodynamic database as Supplementary material. We have attached a Word document named "Support Information" in the revised version.

**Answers to Reviewer # 2 comments:**

This paper provides original carbon window data for WC-Fe-Co-Ni hardmetals at the binder composition of Co:Fe:Ni=40:20:40. The experimental result is valuable but a revision is necessary for a final publication. The detailed comments are in the following:

1. **About the DSC experiment: to our experience, a deviation may exist in the DSC equipment. This deviation leads to generally higher or lower values than the real temperature at which the signal appears. Since the deviation may be more than 10 K, this influence on the final result should be considered. So we suggest a calibration process for the DSC by using a standard sample, i.e. pure metals, compounds, or eutectic mixture with a fixed incipient melting temperature close to that of targeted samples.**

**Answer:** Yes. We have made a calibration process for the DSC by using a pure metal. Temperature calibrations were performed on Ni pure metal with the rates of 10, 5 and 2 °C/min, showing a variation within ±1 °C. The measured value was compared with the theoretical value, which is 1455°C, and the difference between the two values was used for the correction.

2. **In our opinion, the first heating cycle of un-sintered powder mixture regards to an alloying process, the temperature at which the thermal signal appear may not be a real equilibrium. Therefore the tested temperature may deviate a lot from the equilibrium temperature and error bar could be larger. It may be better to consider the second heating ramp of the powder mixture or consider the first heating ramp of the sintered sample as a state more close to the equilibrium transformation.**

**Answer:** We agree with the reviewer's comment. Repeated DSC experiments were carried out without opening the furnace chamber and always protected with pure Argon atmosphere (nominal oxygen and water contents in this gas are 2 ppm and 3 ppm respectively). Of course, the procedure includes leak testing and 3 purges of the calorimeter chamber to remove all residual air (the whole process takes 1. 5 hours). In all cases, the heating and cooling cycles was repeated thrice. Since the first heating ramp of un-sintered powder mixture regards to an alloying process, the temperature at which the thermal signal appear may not be a real equilibrium, the onset temperature of the third heating ramp was considered as the liquid-phase formation temperature in the present work. A paragraph has been included in Section 2 of the revised version and marked it in blue.

3. **About the calculation, many ternary parameters have been revised compared to report by Lengauer et al. [8], which may result in many changes in ternary or quaternary equilibria. The authors should calculate enough ternary and quaternary phase diagrams (with comparisons to experimental data) to validate the modeling for the sub-systems.**

**Answer:** We definitely agree with the reviewer's comment. In the new version, we have included new Figures (Fig. 4, Fig.5, Fig. 6 and Fig. 7) and a new Table (Table 6) corresponding to the calculation of ternary and quaternary phase diagrams, with comparisons to Lengauer`s experimental data, to validate the database. New paragraphs, marked it in blue, has been included in Section 5.3 of the revised version that provides the requested information.

4. **According to figure 4, it seems that the authors prepared 20 hardmetals with five different binder compositions, but the fit is not good for figure 4(c-e) in view that the DSC signals for the incipient melting refers to the solidus instead of liquidus. Table 1 shows that only four hardmetals with one binder composition are prepared in the present work. More experimental details are suggested to be described.**

**Answer:** It has been prepared over 10 different compositions in order to define with precision the compositional ranges free of precipitation of undesired phases. A selection of 4 alloys are included in Table 1 since in the case of alloys 1 and 4 the W or C content was adjusted to ensure the appearance of $M_6C$ or graphite respectively. The other compositions included in Table 1 are those corresponding to the upper (alloy 3) and lower (alloy 2) bounds of the corresponding C windows. The 10 compositions have the same binder composition. We have not prepared 20 compositions with five different binder content. The binder content was 14.3±2 wt%. The binder content has a standard desviation of ±2 since it has to be taken into account that, in all cases, a certain amount of W is dissolved in the binder phase during sintering depending on the C activity [J. Garcia, V. Collado Ciprés, A. Blomqvist, B. Kaplan, Cemented carbide microstructures: a review, Int. J. Refract. Met. Hard Mater. 80 (2019) 40–68]. W dissolution in the metallic binder follows the trend described for WC-Co hardmetals; the larger the carbon loss induced during sintering, the larger the amount of tungsten dissolved in the metallic phase. However, the precipitation of η phase $M_6C$-type carbides or free C decrease the metallic content.
For all of the mentioned above, in Fig. 8 we have had to take into the account the standard desviation of the metallic content to show the different possibilities.

5. **The Figure 5 presents five calculated vertical sections for quinary alloys together with Lengauer's data. However, it seems that the general deviation between cal. and exp. on some sections are larger than the result given by Lengauer. The database should be improved by more careful assessment from sub-systems to quinary systems.**

**Answer:** We appreciate the reviewer comment. The assesments of lower order systems has been included in the revised version in section 5.3. We would like to point out that the measured melting temperatures from Lengauer`s data lie close to the calculated melting range of our database. Also, exact comparisons are not easy. More experiments are being carried out to analyze the C-window and melting temperatures of ternary, quaternary and quinary systems with

different Fe:Ni:Co ratios and different binder contents. We expect to obtain reliable calculations using this new thermodynamic description.

## Answers to Reviewer # 3 comments:

The paper presents an experimental and theoretical work on the phase diagrams calculation of W-C-Co-Fe-Ni system. The validation of the thermodynamic model with experimental data shows a very good accord in terms of the liquid phase formation temperatures in this study and other works from the literature. This thermodynamic study has very good scientific quality and is of clear interest for the cemented carbide community.

**1. The C window is not accurately determined in Fig.4, namely for higher binder contents, as stated in the text and conclusions. Please, revise these sentences.**

**Answer:** We appreciate the reviewer comment. We have revised these sentences and marked it in blue in the revised version.

**2. The determination of the onset temperatures from DSC curves would be clearer by adding the constructions lines.**

**Answer:** We agree with the reviewer's comment. In the revised version, we have added in Fig. 2 the construction lines.

## HIGHLIGHTS

1- The liquid phase formation temperatures of WC-FeCoNi alloys with a ratio of Fe:Co:Ni=40:20:40 were measured by DSC.

2- The C-window of WC-FeNiCo alloys with a ratio of Fe:Co:Ni (in wt.%)=40:20:40 was defined accurately.

3- Temperature-composition sections of the W-C-Co-Fe-Ni system with different binder contents and different Fe:Co:Ni ratios were provided.

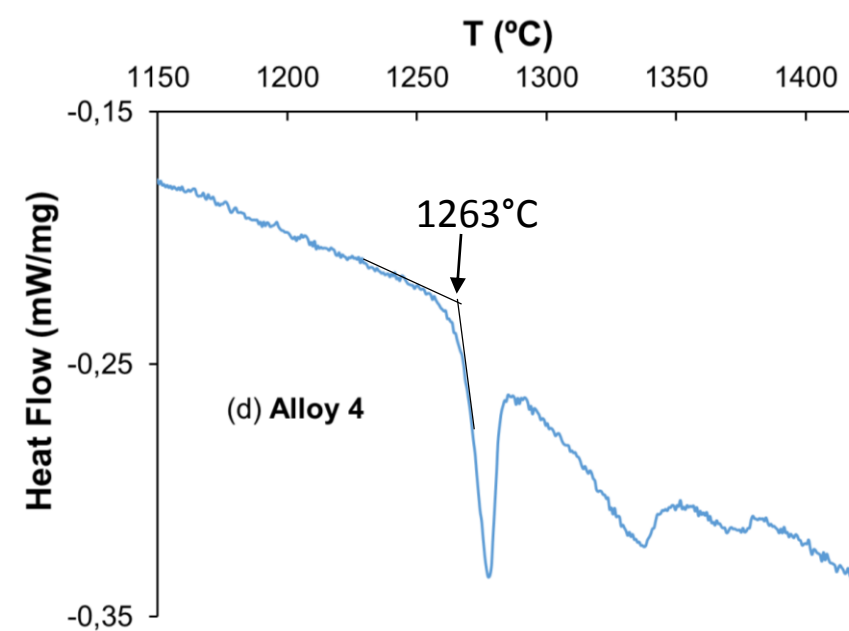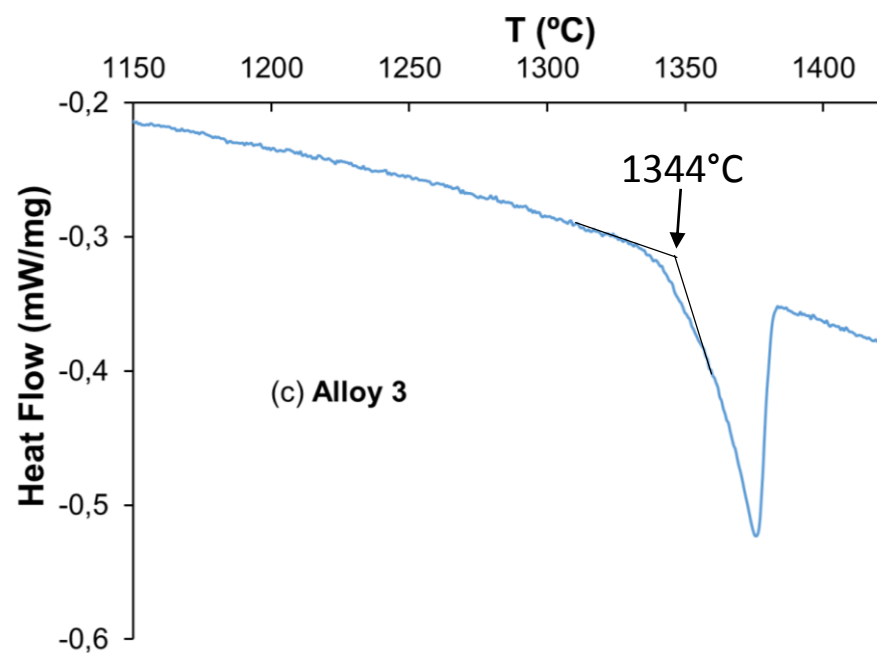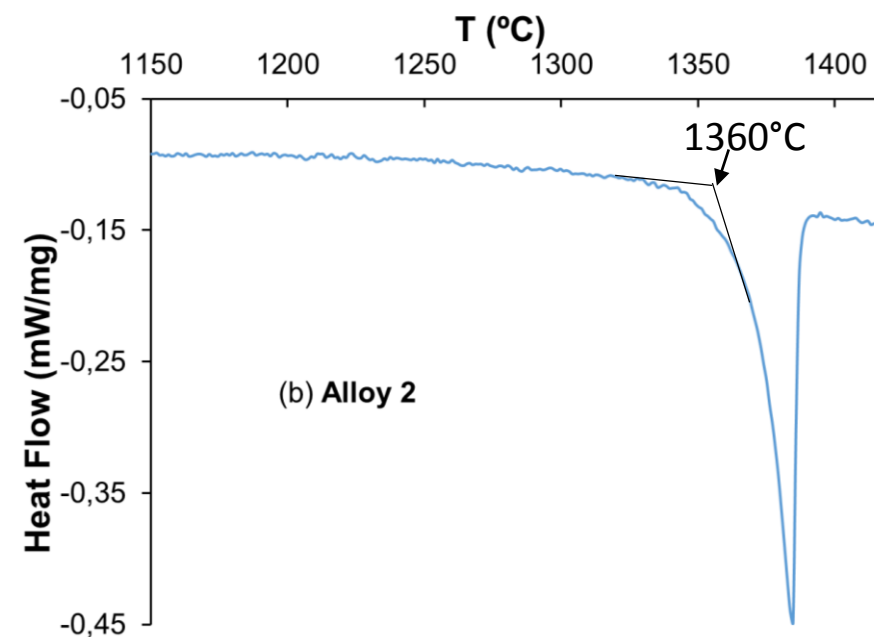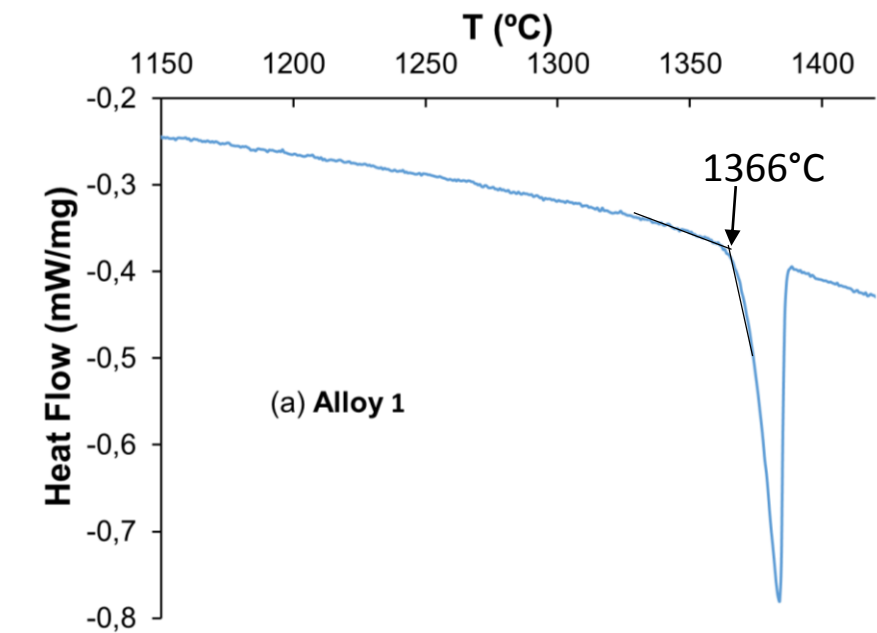4- The experimental results are well reproduced by the present modelling.
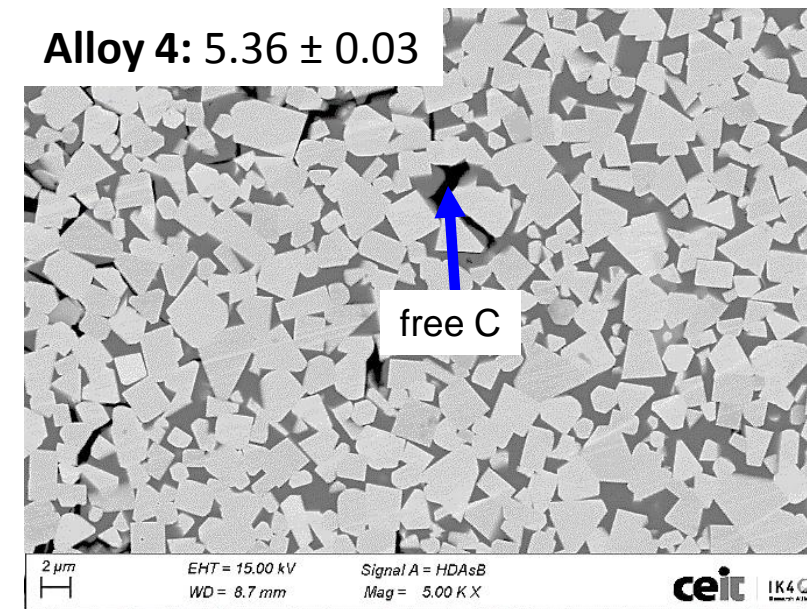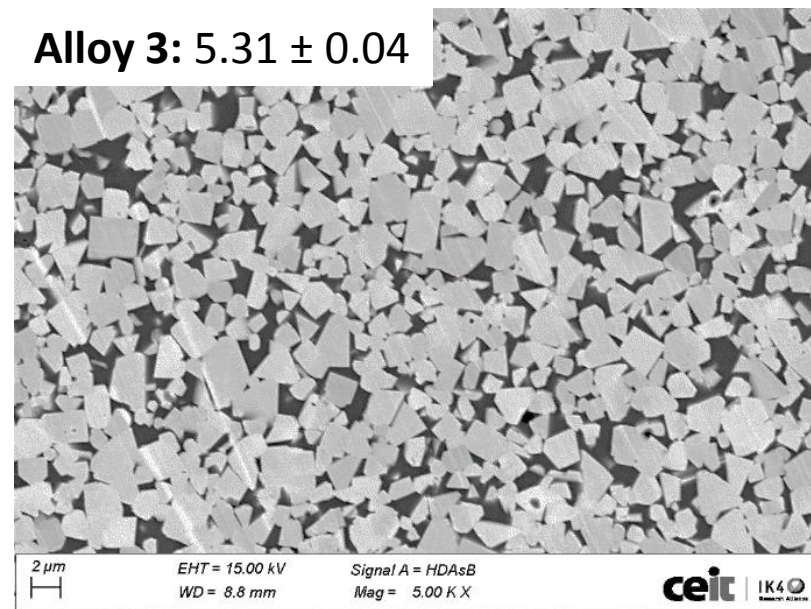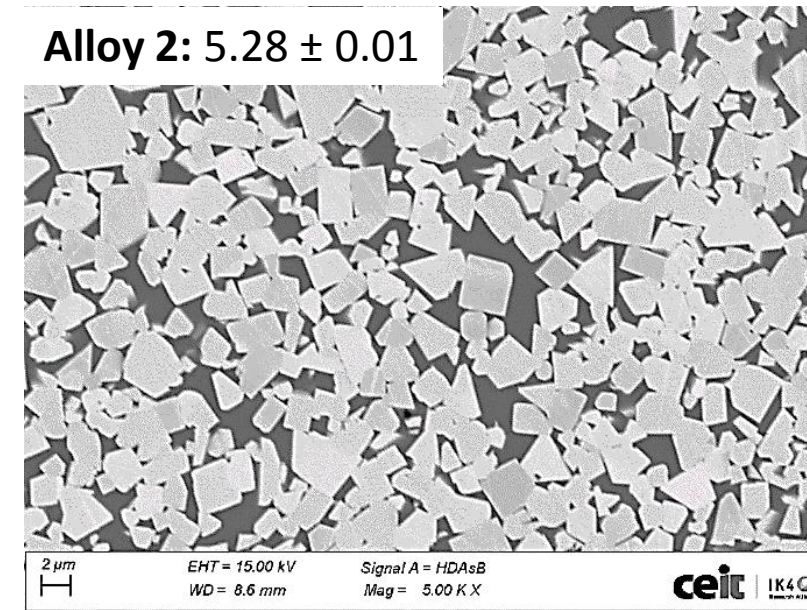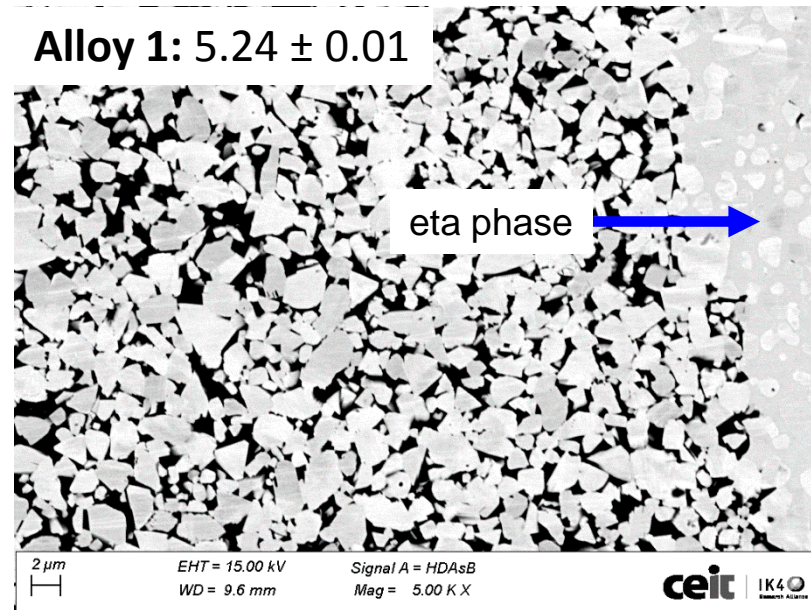
Figure 1
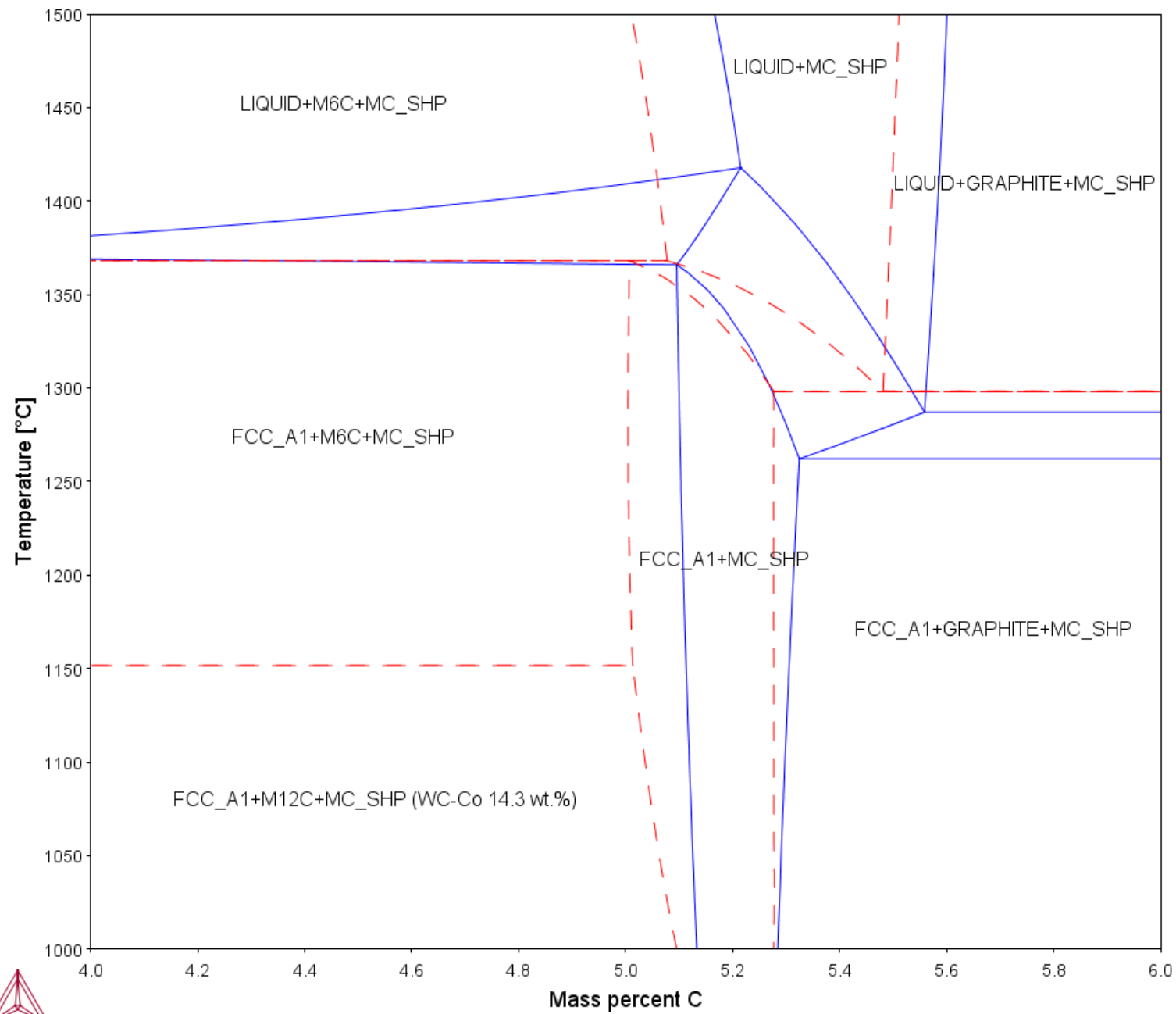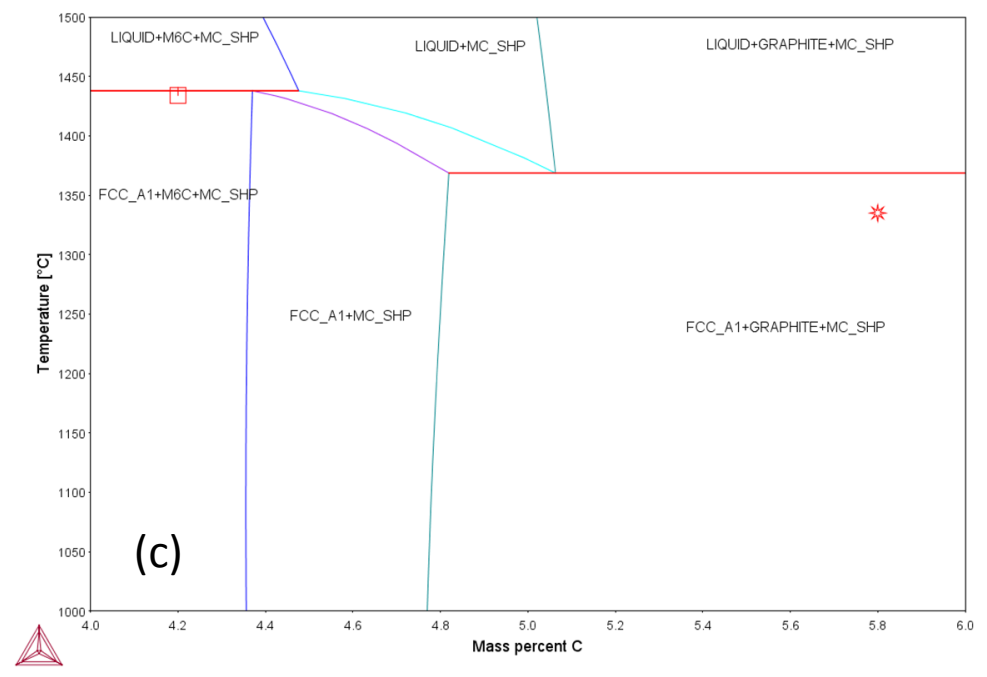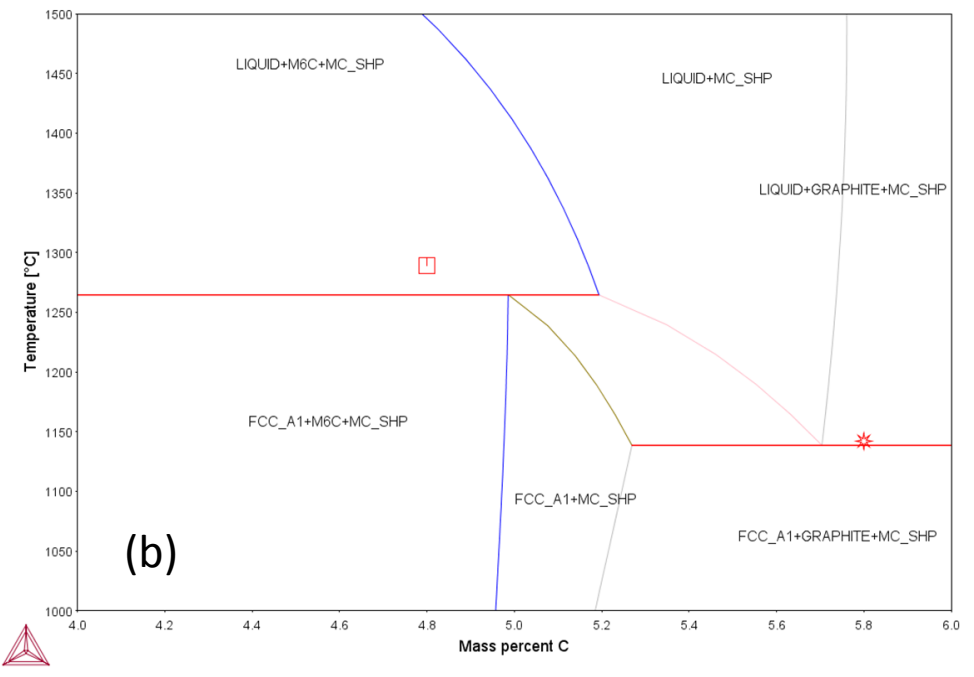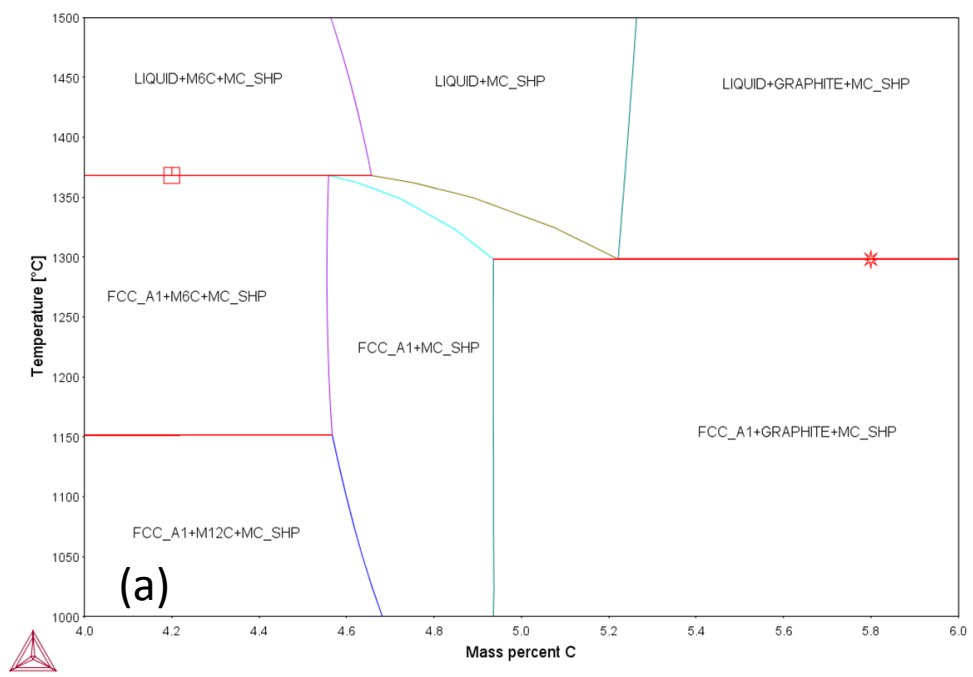
Figure 2
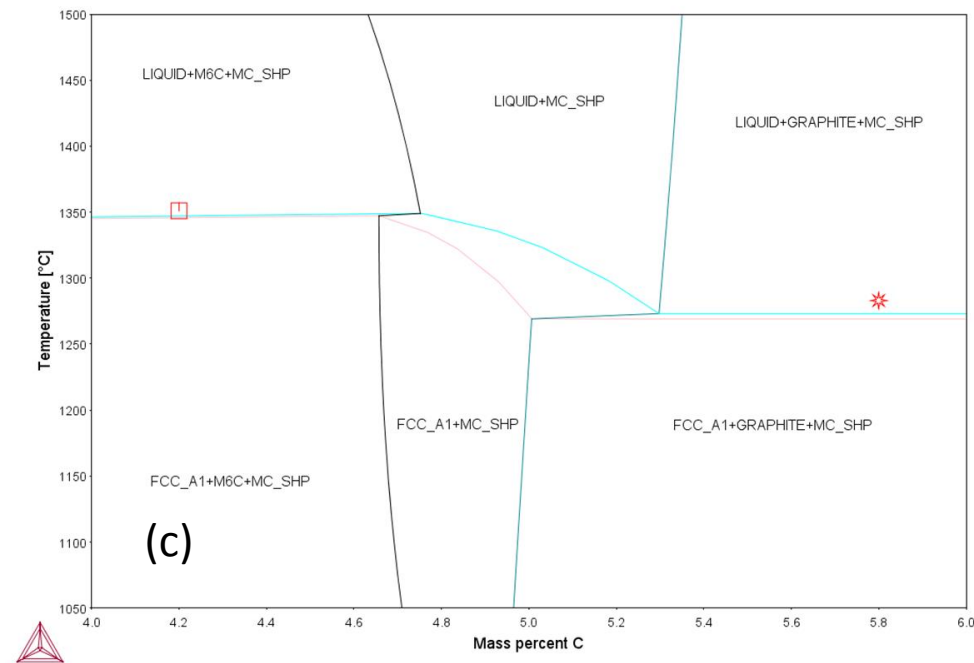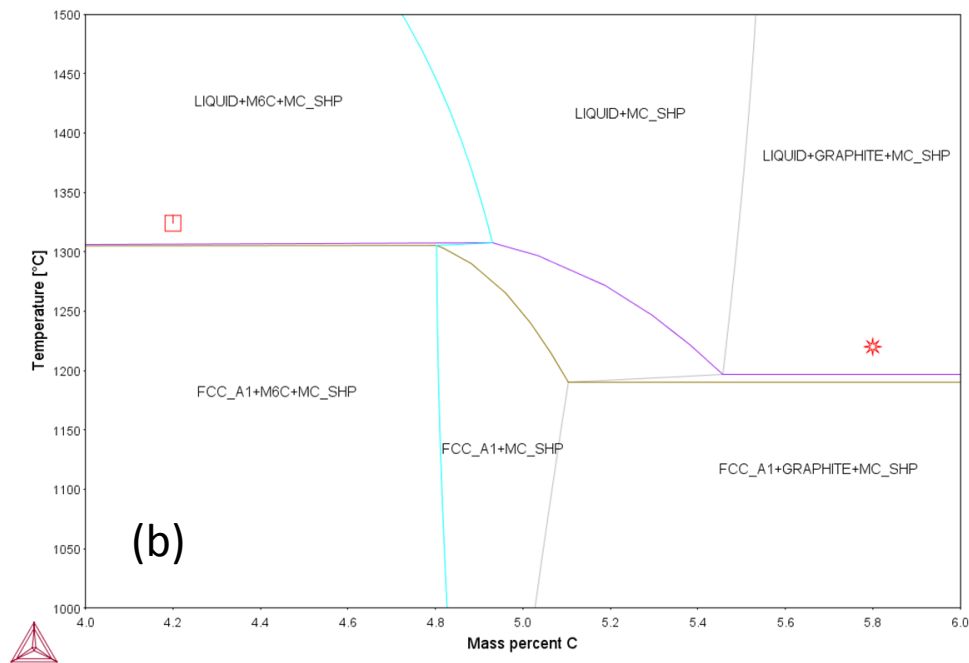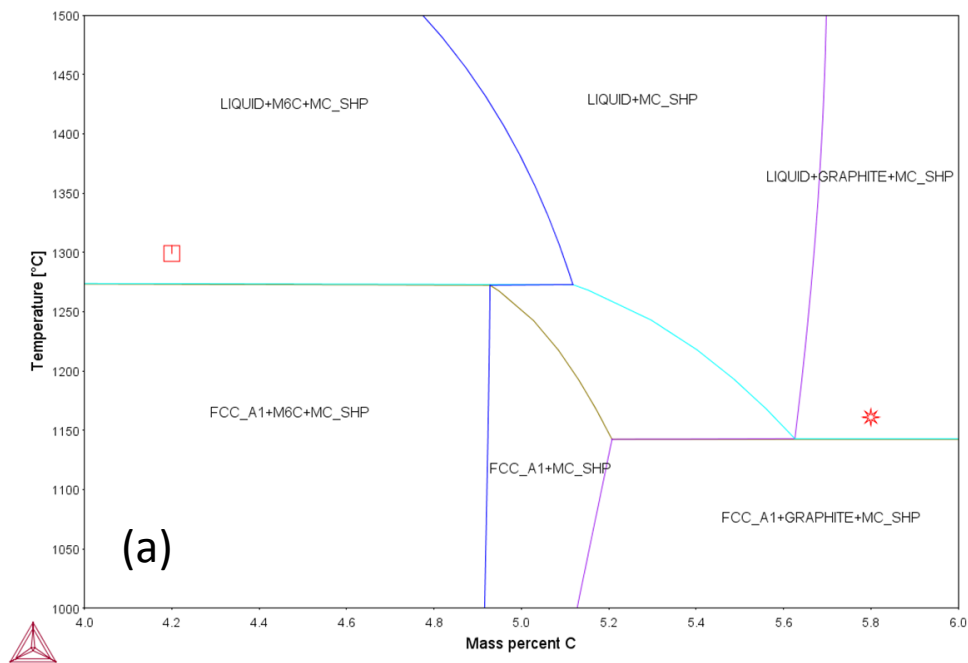
Figure 4

Figure 5

Figure 6
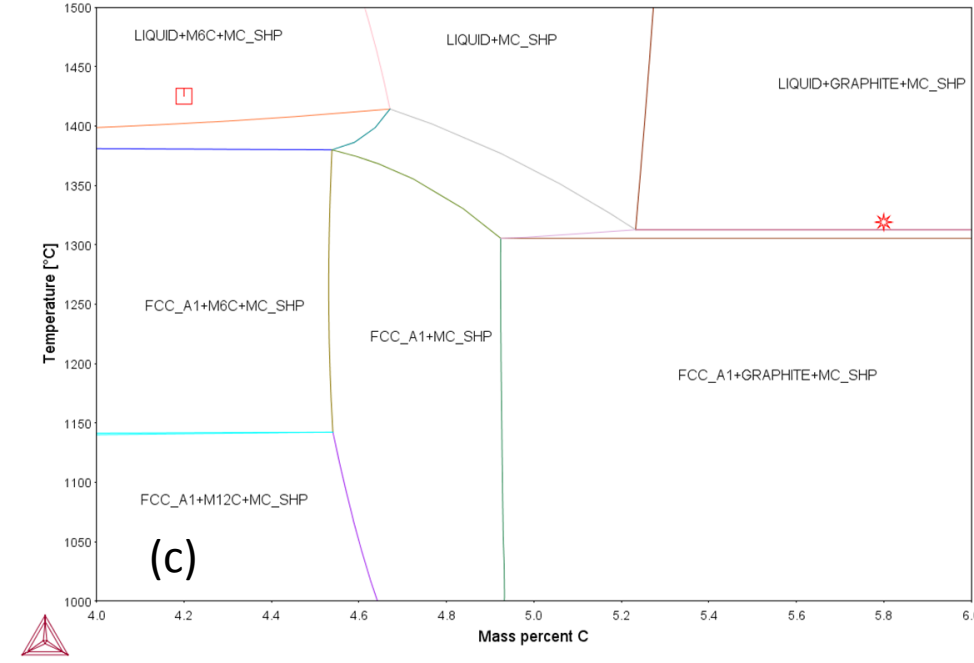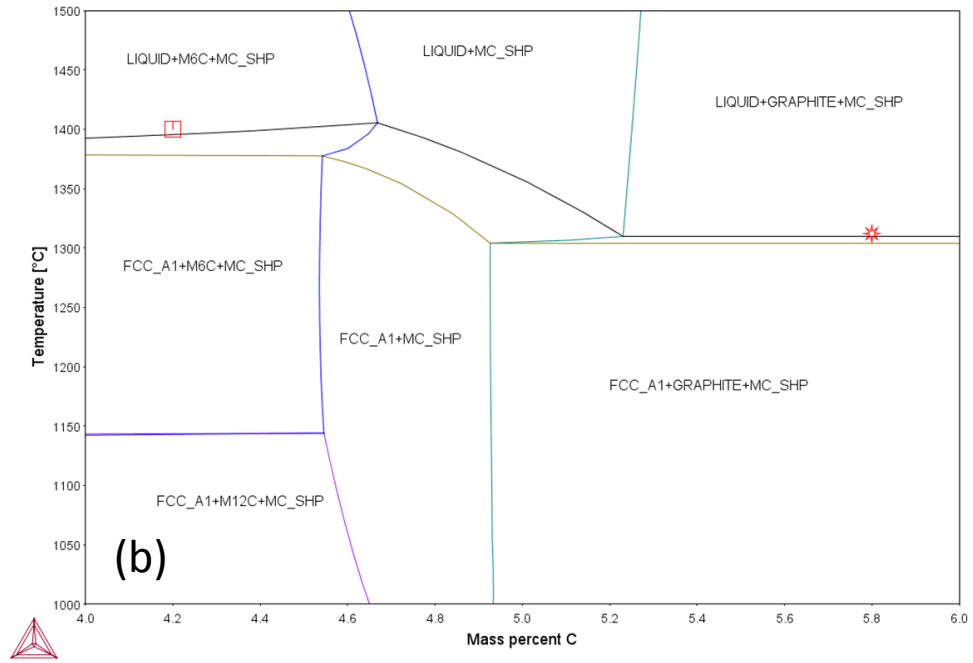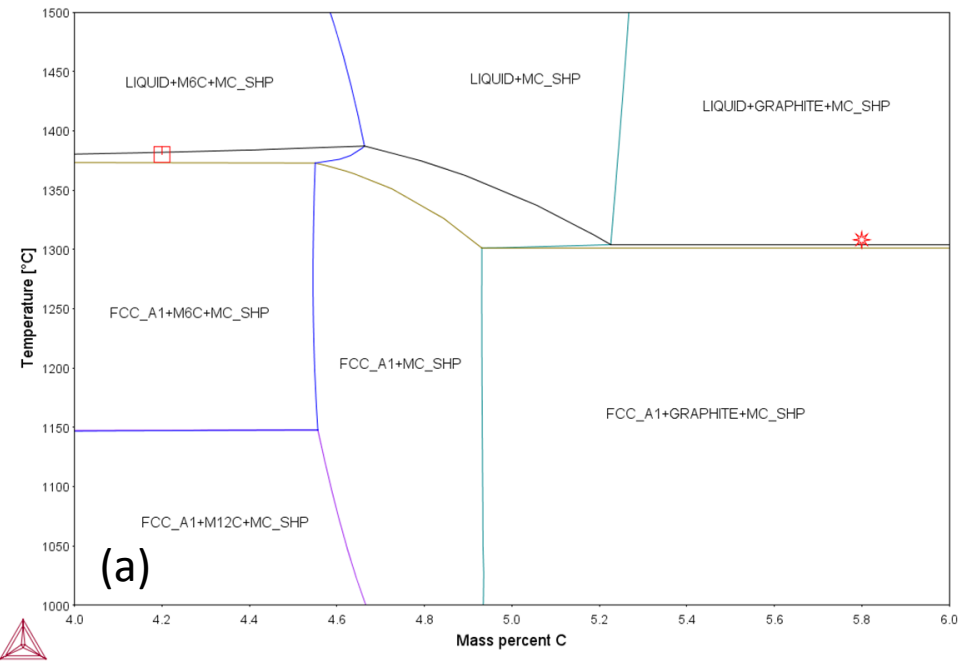
Figure 7
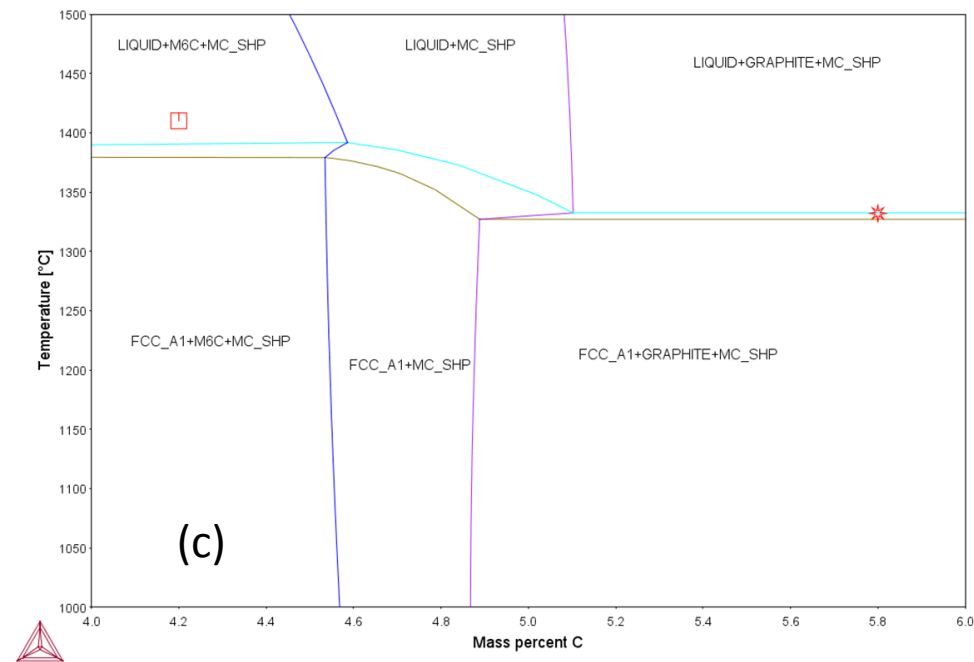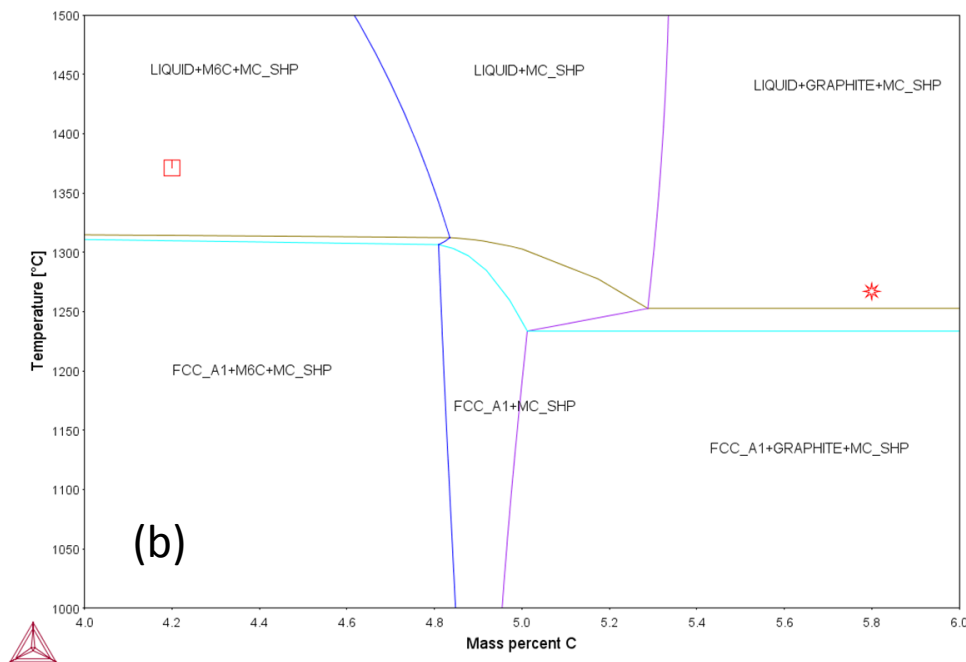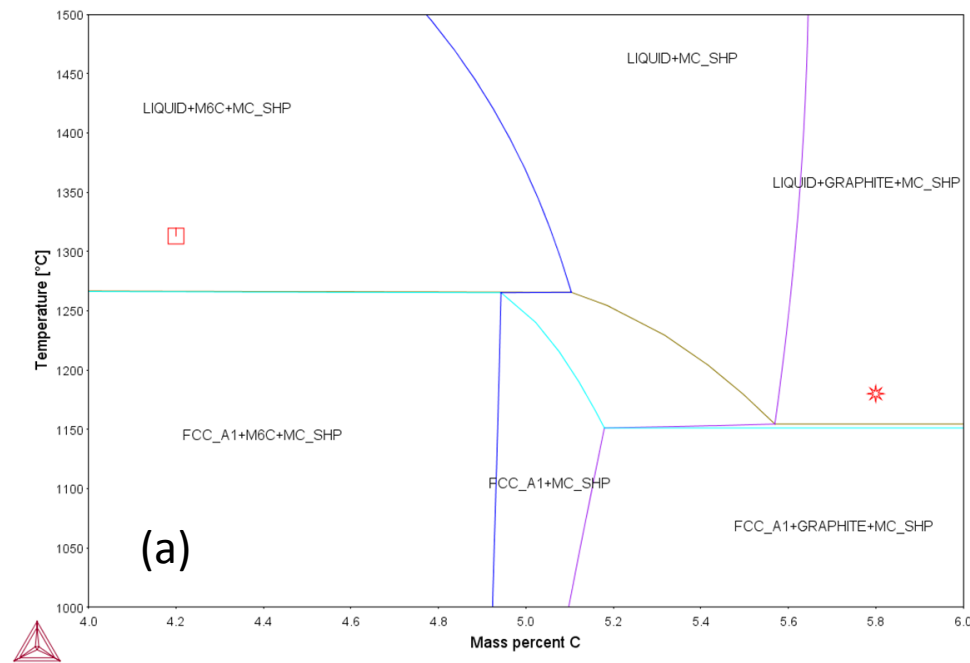
Figure 8
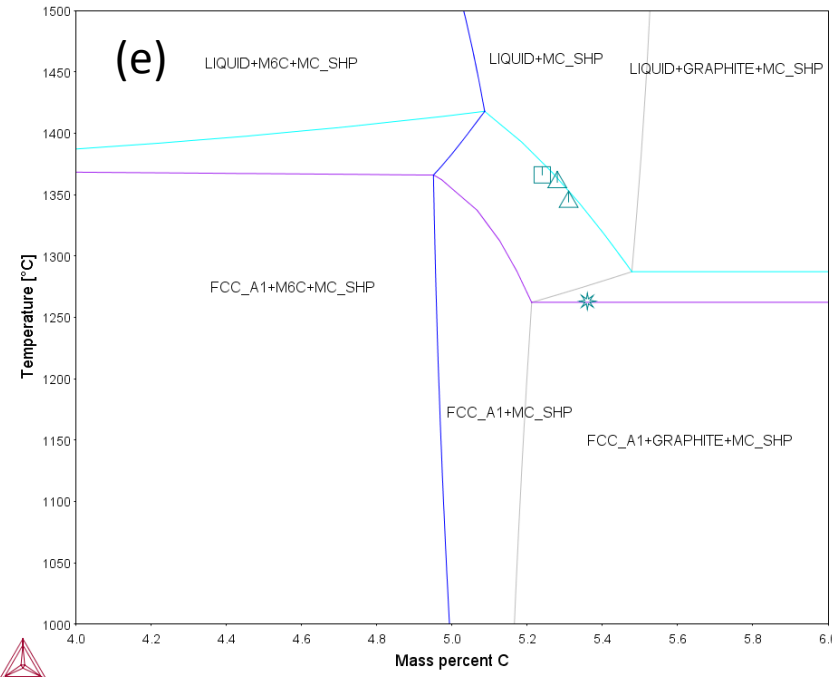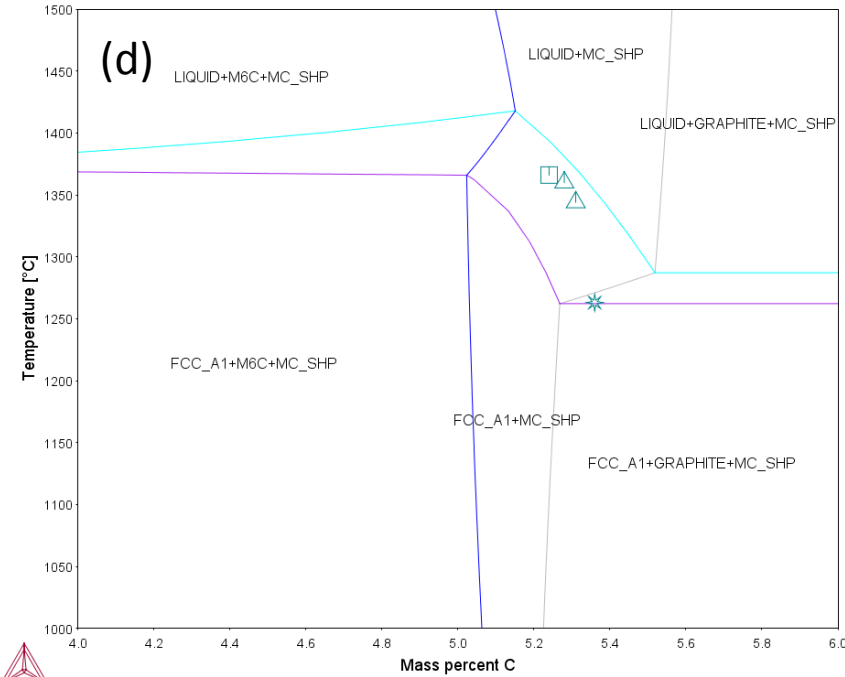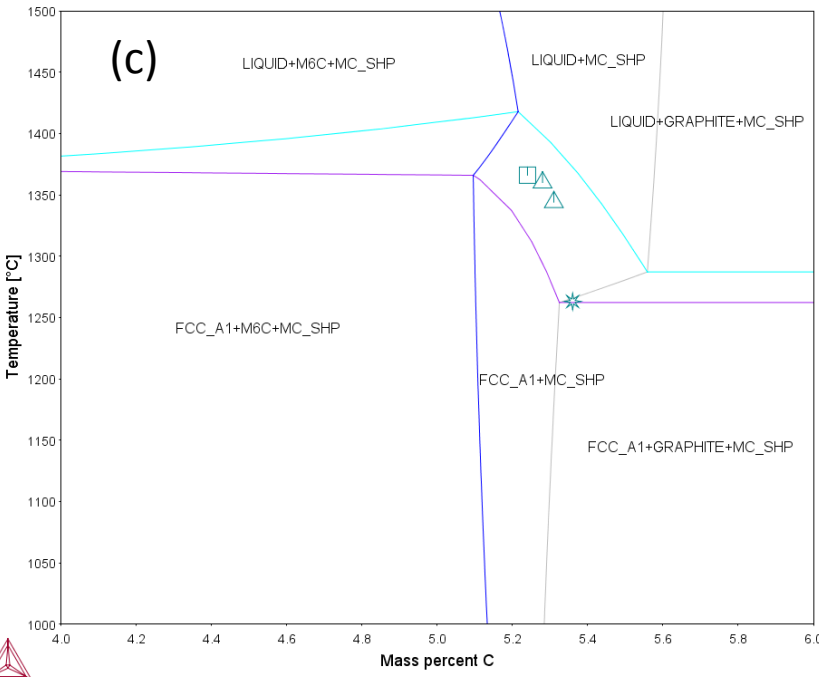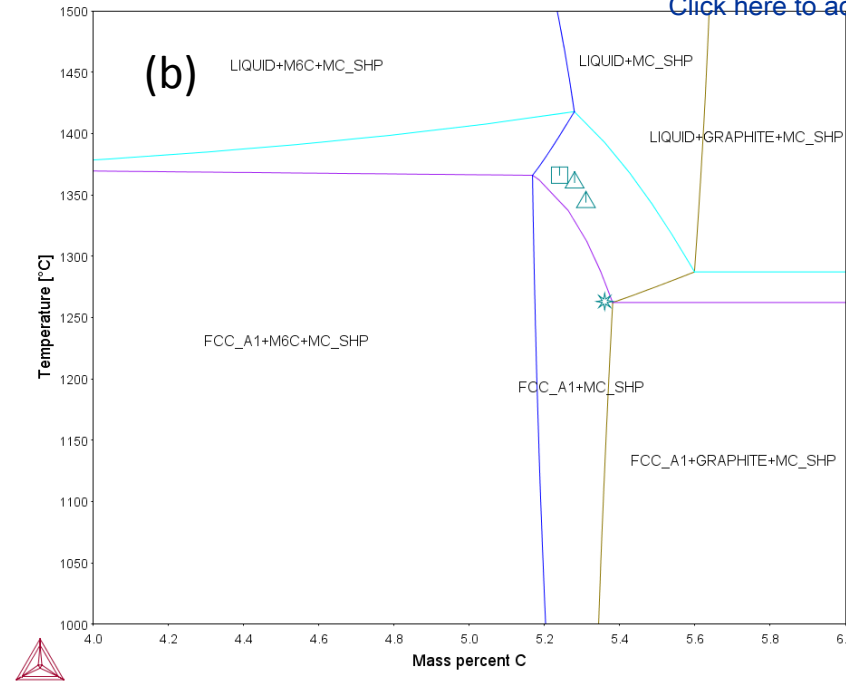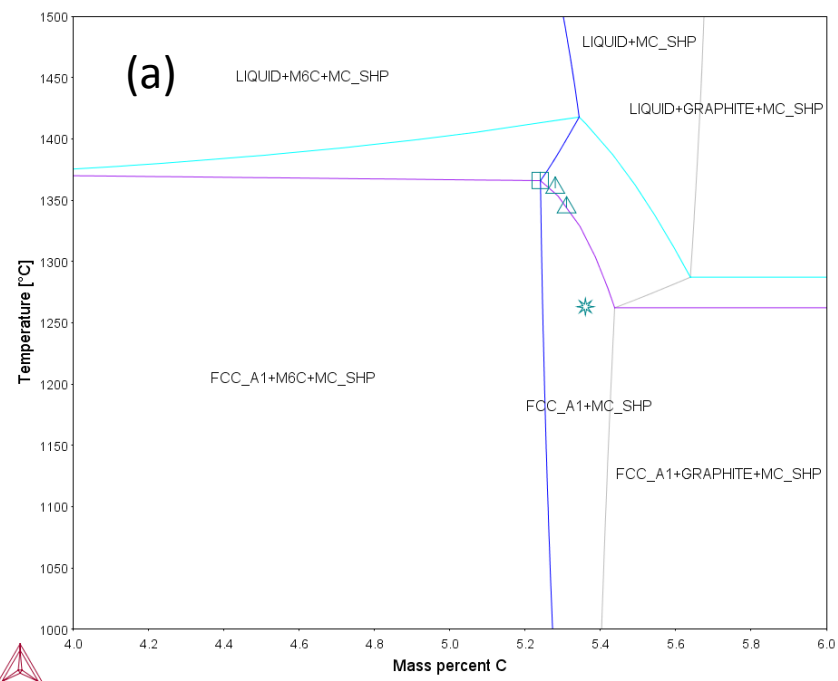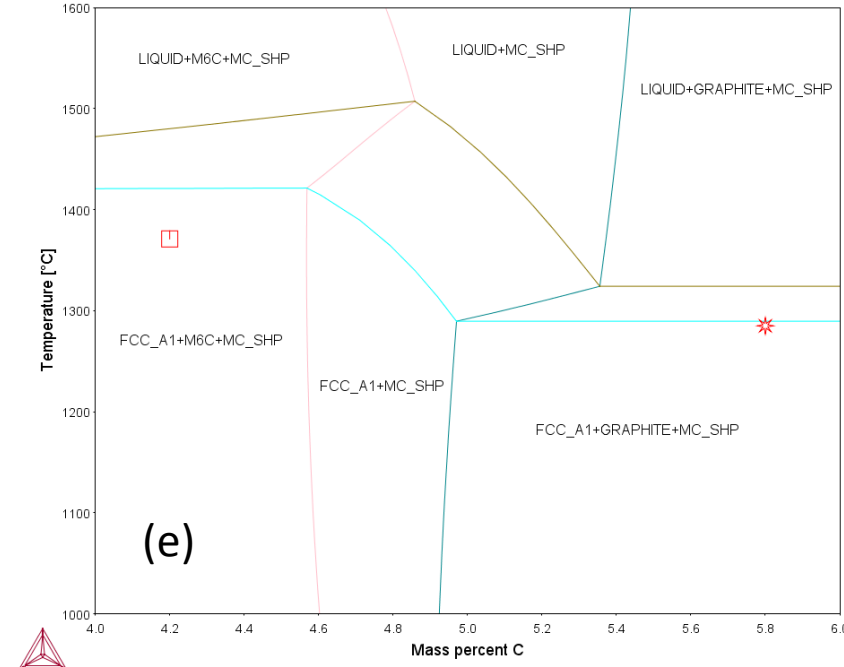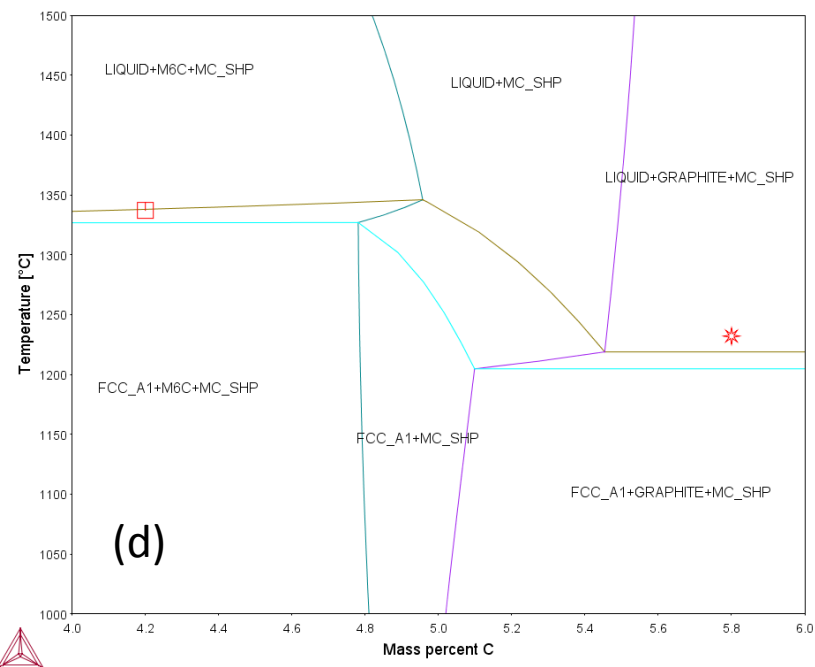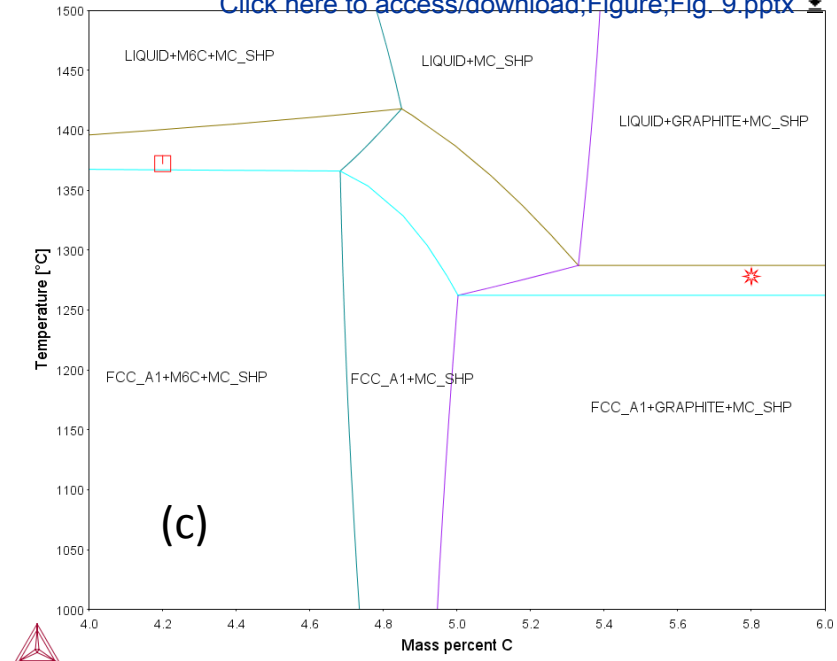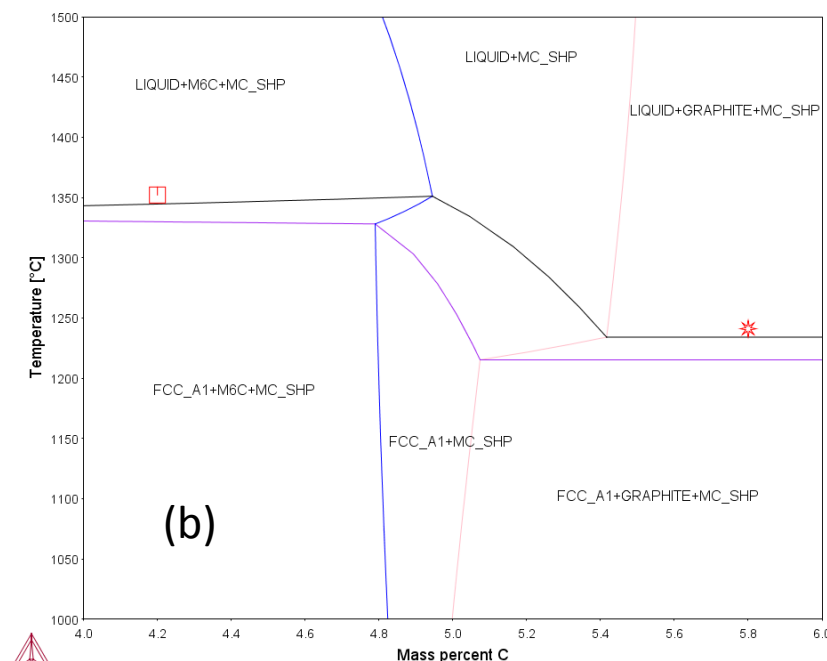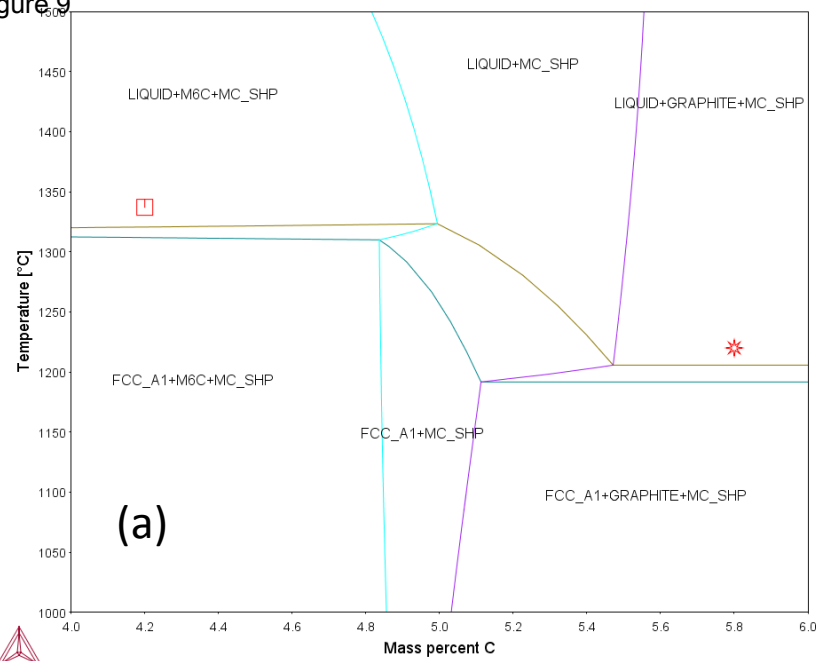
Figure 9

**Declaration of interests**

☒ The authors declare that they have no known competing financial interests or personal relationships that could have appeared to influence the work reported in this paper.

☐ The authors declare the following financial interests/personal relationships which may be considered as potential competing interests:

Corresponding author on behalf of all coauthors

Tomas Soria-Biurrun

Dear Editor,
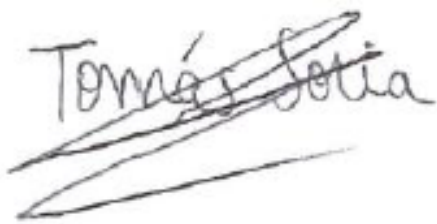
We the undersigned declare that this manuscript entitled "Experimental and theoretical study of WC-40Fe-20Co-40Ni" is original, has not been published before and is not currently being considered for publication elsewhere.

We confirm that the manuscript has been read and approved by all named authors and that there are no other persons who satisfied the criteria for authorship but are not listed. We further confirm that the order of authors listed in the manuscript has been approved by all of us.

We understand that the Corresponding Author is the sole contact for the Editorial process. He is responsible for communicating with the other authors about progress, submission of revisions and final approval of proofs.

On behalf of the corresponding author

Tomas Soria-Biurrun

**Experimental and theoretical study of WC-40Fe-20Co-40Ni**

Tomas Soria-Biurrun[1,2] tsoria@ceit.es, Jose M. Sánchez-Moreno[1,2] jmsanchez@ceit.es, Karin Frisk[3,4] friskk@chalmers.se

1- CEIT-Basque Research and Technology Alliance (BRTA), Manuel Lardizabal 15, 20018 Donostia /San Sebastián, Spain.

2- Universidad de Navarra, Tecnun, Manuel Lardizabal 13, 20018 Donostia / San Sebastián, Spain.

3- Chalmers University of Technology, Industrial and Materials Science, SE-412 96 Gothenburg, Sweden.

 4- Höganäs AB, SE-263 83 Höganäs, Sweden.

**Abstract**

The liquid phase formation temperatures of the quinary system W-C-Co-Fe-Ni with a ratio of Fe:Co:Ni = 40:20:40 were determined by means of DSC analysis. Besides, the experimental C-window of this system with a binder content of 14.3 ± 2 wt.% is accurately defined. Based on the experimental results, a thermodynamic modelling is carried out using the CALPHAD approach. Temperature-composition sections of the W-C-Co-Fe-Ni system with different binder contents are calculated to verify the rationality of the present modelling. There is a good correlation between the experimental and calculated results showing that the experimental data can be well reproduced by the present modelling.

**1. Introduction**

It is well known that partial or total substitution of Co in cemented carbides is an important issue for the hardmetal industry [1]. Among these alternative cemented carbides, those based on WC-Fe-Ni-Co powder mixtures have been extensively studied due to their good combination of fatigue strength and fracture toughness [2,3]. According to different authors, larger carbon windows are obtained by combining Fe, Ni and Co, especially for compositions within the austenitic range [4, 5].

Among them, the alloy consisting of 40wt.%Fe-40wt.%Ni-20wt.%Co is one of the most promising due to its relatively wide C window and its high toughness compared with other Fe-Ni-Co based compositions [4].

Guillermet [6] established a thermodynamic database of the Co-Fe-Ni-W-C system. However, his results need more experimental data to improve the accuracy of this database [7].

Lengauer et al. [8] have constructed a thermodynamic description of the W-C-Co-Fe-Ni system by applying the Calphad approach to provide a general revision for the C-Co-Fe-Ni-W database. They study the four-phase equilibria, i.e., $L + WC + fcc + M_6C$ and $L + WC + fcc + graphite$, and give maximum and minimum melting temperatures of binders for favourable hardmetals within the WC + fcc window.

Nevertheless, few experimental data on the two four-phase transformations, C-window and mechanical properties in the C-Co-Fe-Ni-W system are available in the literature. Thus, in the present work the main goal is to focus on the quinary system C-Co-Fe-Ni-W with a binder content of 14.3 ± 2 wt% and a ratio of Fe:Co:Ni = 40:20:40. The microstructure of the alloys and their correspondence liquid phase formation temperatures are given, not only for the four-phase equilibria, i.e., $L + WC + fcc + M_6C$ and $L + WC + fcc + graphite$, but also for the three-phase equilibria, i.e., L + WC+ fcc, that corresponds to the alloys within the C-window. Besides, a study of the effect of binder content on the carbon window which is defined precisely and it is very important for industrial processing. Finally, the thermodynamic parameters of Guillermet and Lengauer et al. [6,8] were studied thoroughly to provide a new thermodynamic description for this quinary system.

## 2. Experimental procedure

Over 10 different compositions have been prepared with these materials in order to define with precision the compositional ranges free of precipitation of undesired phases. A selection of 4 alloys are included in Table 1. In the case of alloys 1 and 4 the W or C content was adjusted to ensure the appearance of $M_6C$ or graphite respectively. The other compositions included in Table 1 are those corresponding to the upper (alloy 3) and lower (alloy 2) bounds of the corresponding C windows. The total metallic content was 14.3 ± 2 wt%. The ratio between Fe, Ni and Co was 40/40/20 (in wt%) in all cases. Powder processing and sintering of these materials have already been described elsewhere [9]. C contents were measured by means of infrared spectrometry both

in green compacts and sintered materials. Standard ISO 3369 was used for density measurements. Sintered specimens were ground and polished down to 1 μm diamond paste for microstructural analysis, which was carried out by optical and scanning electron microscopy (FEG-SEM) and energy dispersive X-ray spectroscopy (EDS). For each DSC analysis, about 100–150 mg of mixed powder was used. The powder was pressed into an $Al_2O_3$ crucible,which was then subjected to DSC investigations using a TGA/DSC Setaram Setsys Evolution 16/18. DSC samples were cubes of aprox. 1 mm side. The heating cycle consisted of a heating ramp of 10 °C/min up to 1450 °C. Dwelling time at this temperature was 10 min. Argon at atmospheric pressure was used as a protective atmosphere. The onset temperature is known as the intersection between the extrapolated base line and endothermic peak onset, indicating the liquid-phase formation in the sample. In all cases, the heating and cooling cycles was repeated thrice. Since the first heating ramp of un-sintered powder mixture regards to an alloying process, the temperature at which the thermal signal appear may not be a real equilibrium, the onset temperature of the third heating ramp was considered as the liquid-phase formation temperature in the present work.

## 3. Thermodynamic models

In the present modelling, the Gibbs Energy functions for pure elements C, Co, Fe, Ni, and W are taken from the SGTE compilation by Dinsdale [10]. The liquid phase is described by a substitutional solution model, and its Gibbs Energy expression is described by the following polynomial [11]:

$$G_m^L = \sum_i x_i \, G_i^L + RT \sum_i x_i \, lnx_i + \sum_{i \neq j} x_i \, x_j L_{i,j}^L + \sum_{i \neq j \neq k} x_i x_j x_k L_{i,j,k}^L + \sum_{i \neq j \neq k \neq l} x_i \, x_j x_k x_l L_{i,j,k,l}^L \qquad (1)$$

where $R$ is the gas constant, $x_i$ , $x_j$ , $x_k$ , and $x_l$ (*i*, *j*, *k*, and *l* represents C, Co, Fe, Ni, and W) are the mole fraction of elements *i*, *j*, *k*, and *l*, respectively. The standard element reference (SER) state, i.e., the stable structure of the element at 25 °C and 1 bar, is used as the reference state of Gibbs Energy.

$L_{i,j}^L$, $L_{i,j,k}^L$, and $L_{i,j,k,l}^L$ are the binary, ternary, and quaternary interaction parameters, respectively. The *L* parameters can be composition dependent, usually only in ternary systems and then will be defined by:

$$L_{i,j,k} = \ x_i L^1 + x_j L^2 + x_k L^3 \qquad (2)$$

The solid solution phases are described using sublattice models developed by Hillert and Staffansson [12]. A solid solution phase may be described with the two-, three-, or four-sublattice model based on its crystallography. Taking the two-sublattice $(Co,Fe,Ni,W)_a(C,Va)_c$ as an example, the first sublattice is a substitutional one occupied by Co, Fe, Ni, and W atoms, while the second sublattice is an interstitial one occupied by C atoms and vacancies. The symbols a and c denote the amounts of sites on each sublattice and have values of a = 1 and c = 1 for the fcc phase, a = 1 and c = 3 for the bcc phase, and a = 1 and c = 0.5 for the hcp phase. For one formula unit of $(Co,Fe,Ni,W)_a(C,Va)_c$, the Gibbs Energy is expressed as follows:

$$G_m^\phi = \sum_i (y_i' y_C'' G_{i:C}^\phi + y_i' y_{Va}'' G_{i:Va}^\phi) + RT(a\sum_i y_i' lny_i' + cy_c'' lny_c'' + cy_{Va}'' lny_{Va}'') + \sum_i y_i' y_C'' y_{Va}'' L_{i:C,Va}^\phi +$$

$$\sum_{i\neq j} y_i' y_j' y_C'' L_{i,j:C}^\phi + \sum_{i\neq j} y_i' y_j' y_{Va}'' L_{i,j:Va}^\phi + \sum_{i\neq j} y_i' y_j' y_C'' y_{Va}'' L_{i,j:C,Va}^\phi + \sum_{i\neq j\neq k} y_i' y_j' y_k' y_C'' L_{i,j,k:C}^\phi +$$

$$\sum_{i\neq j\neq k} y_i' y_j' y_k' y_{Va}'' L_{i,j,k:Va}^\phi + G_m^{magn,\phi} \tag{3}$$

where $y_i'$, $y_j'$ , and $y_k'$ are the site fractions of *i*, *j*, and *k* (*i*, *j*, *k* represents Fe, Co, Ni, or W) in the first sublattice, and $y_C''$ and $y_{Va}''$ are the site fractions of C and Va in the second sublattice. The parameter $G_{i:Va}^\phi$ is the Gibbs Energy of pure element *i*, and the parameter $G_{i:C}^\phi$ is the Gibbs Energy of a hypothetical state where all the interstitial sites are completely filled with C. $L_{i,j:Va}^\phi$ or $L_{i:C,Va}^\phi$ is a binary interaction parameter from the *i-j* or *i*-C sub-system. $L_{i,j:C}^\phi$ or $L_{i,j,k:Va}^\phi$ is a ternary interaction parameter from the C-*i-j* or *i-j-k* sub-system. $L_{i,j,k:C}^\phi$ is a quaternary interaction parameter from the C-*i-j-k* sub-system. $G_m^{magn,\phi}$ is the magnetic contribution to the Gibbs energy.

## 4. Thermodynamic assessment

The thermodynamic parameters of liquid is adjusted by using the experimental data of the present DSC measurement. Each DSC value was given an equal weight due to the same experimental condition. Since the assessment covers a large number of sub-systems in the C-Co–Fe-Ni-W quinary system, a step-by-step modelling is explained as the following.

Firstly, the thermodynamic parameters of sub-systems from the following literature, C-Co [13], C-Fe [14], C-Ni [15], C-W [16], Co-Fe [17], Co-Ni [18], Co-W [19], Fe-Ni [20], Fe-W [21], Ni-W [22], C-Co-Fe [23], C-Co-Ni [24], C-Co-W [19], C-Fe-Ni [25], C-Fe-W [26], Co-Fe-W [27], C-Ni-W [22], Co-Ni-W [6, 8] , Fe-Ni-W [28], C-Co-Fe-W [6], C-Co-Ni-W [6, 8] and C-Fe-Ni-W [29], were collected to establish a preliminary thermodynamic database.

Secondly, the assessment was conducted in the liquid phase by changing one by one the values and using the Lengauer parameters [8]. By this procedure it was shown that the Gibbs energies of liquid phase of Co,Ni,W and C,Co,Ni,W are the most important, and by adding only these from [8], the calculated results fit pretty well.

Finally, the DSC values C-Co-Fe-Ni-W alloys were taken into account. In this step, the Gibbs energies of liquid phase of Co,Ni,W and C,Co,Ni,W are adjusted to reproduce the present experimental data.

## 5. Results and discussion

### 5.1. Microstructure and thermal analysis

The thermodynamic parameters used in the present work are summarised in Table S1.

Fig. 1 shows the microstructure and the C content (Table 2) of the four compositions, the alloy 1 with eta phase, alloys 2 and 3 within the C-window and alloy 4 with free C.

Fig. 2 shows the heating cycles of the four alloys. From the heating cycles, the melting onset is obtained (Table 2). Table 2 shows the displacement of melting onset to higher temperatures as C activity decreases, this is a well-known effect in cemented carbides.

Table 3 presents the calculated temperatures of the four-phase transformations taking into account the thermodynamic parameters of Table S1 together with the presently measured DSC values (Table 2). The agreement of the present calculations with the experiments is excellent. In addition, these results are compared with the Lengauer data [8] and it can be seen that the values of the liquid phase formation in the four-phase transformation are pretty similar, and lie within the experimental uncertainties.

### 5.2. Binder content, C-window and melting onset

Tables 4 and 5 compare the calculated values of melting onset and C-window of the quinary system W-C-Co-Fe-Ni with different binder contents and with a ratio of Fe/Ni/Co = 40/40/20 using different databases. This comparison shows the importance of the binder content in the obtained values for the calculated C-window. It shows the shift to lower C contents when the binder content increases. Furthermore, when the binder content increases, the width of the carbon window increases as it can be shown in Tables 4 and 5. Therefore, when the binder content increases is less difficult to obtain materials that fulfil the requirement on the C-window. It is vital to define precisely the C-window to avoid secondary carbides or undesirable phases. In addition, it is

important to take into account the loss of carbon in the sintering process. For this reason, it is useful to have access to accurate calculations to predict the C-window.

The importance of the C-window and the binder content was experimentally verified by Schubert et al. [4] who compared the C-window of the Fe-Ni-Co-W-C system with different ratios of Fe:Ni:Co. In the case of Fe:Co:Ni = 40:20:40 at Fe + Co + Ni = 10 wt%, the C-window is 0.09 which is narrower than the C-window obtained with WC–10 wt% Co hardmetals which is about 0.14 (Table 5). In the case of 11.8 wt% binder and Fe:Co:Ni = 40:20:40 the C-window calculated by Schubert et al. is 0.11. These C-window ranges obtained by Schubert et al. agrees with the prediction of C-window range using our database, Lengauer database and TCFE10 database (Tables 4 and 5).

In our case (Tables 4 and 5), at Fe+Co+Ni = 14.3 wt% and Fe:Co:Ni = 40:20:40 the C-window is 0.10, the same range as obtained with calculations using the Lengauer database [8]. However, it is 0.21 when calculated with the Guillermet database [6] and 0.13 when using the TCFE10 database. As shown in Tables 4 and 5, in the case of our database and Lengauer database the C range is the same and it is pretty similar to TCFE10 database and Guillemet database. The difference is in the side of eta phase since the C content is different. Besides, the melting onset in the side of eta phase and free C is higher in our database and the Lengauer database in comparison to the other databases.

Our experimental results (Table 2), not only the C-window (5.24-5.36; $\Delta C = 0.12$) but also the melting onset in both sides (1366 ($M_6C$) and 1263 (Free C)), fit pretty well with the Lengauer database in the case of 14.3 and 13.3 wt.% in binder content (Table 4).

In the case of WC-Co with 13.3 and 14.3 wt% of Co in all the databases the C-window is in the range of 0.20 (Table 5). This means that the width of the C-window is higher in the case of Co binder in comparison to use Fe:Ni:Co = 40:40:20 as binder (Tables 4 and 5). Fig. 3 shows, using the new thermodynamic description, the comparison between the calculated section through the W-C-Co system and W-C-Fe-Ni-Co system at 14.3 wt.% Co and 14.3 wt.% 40Fe-40Ni-20Co. It is obvious the difference in C-window which is wider in the case of Co as binder and also the melting temperature is higher in the free C side. It is well known that Fe as binder reduces the width of the C-window and decreases the melting temperatures [4, 5]. Nevertheless, the C-window in the

case of this system (Fe/Ni/Co = 40/40/20) is quite promising because is wider than other Fe:Ni:Co ratios [4, 30].

## 5.3. Calculated Phase Diagrams

Table S1 shows the thermodynamic parameters that were used to calculate the phase diagrams of the quinary system W-C-Fe-Ni-Co.

Fig. 4, Fig. 5, Fig. 6 and Fig. 7 show ternary and quaternary phase diagrams, with comparisons to Lengauer`s experimental data [8], to validate the modeling for the sub-systems. Besides, Table 6 provides a comparison between the Lengauer`s DSC data and this new thermodynamic description.

Fig. 4 shows the vertical sections of C-Co-W, C-Fe-W and C-Ni-W systems at 20 wt.% binder together with the present experimental results of Lengauer et al. [8]. In the case of the C-Co-W system, the calculated reaction temperatures of the two four-phase equilibria are in good agreement with the experimental DSC values of Lengauer et al. [8]. On the other hand, as it can be seen in the C-Fe-W system, the transformation temperature in the side of free C can be well reproduced, while in the side of $M_6C$ the present calculation shows a slight difference to the DSC value. Regarding the C-Ni-W system, in the side of eta phase, the agreement between the present calculation and the experimental value is quite good. Nevertheless, in the side of free C, there is a slight difference between the predicted value and the experimental value. Fig. 5 presents the calculated vertical section of C-Co-Fe-W system at 20 wt.% binder with Fe:Co = 85:15, 50:50, and 15:85, together with the present experimental results. The experimental values are a little bit higher than the predicted. However, there is a good correlation between the calculated values and the experimental values. Fig. 6 shows the calculated vertical section of the C-Co-Ni-W system at 20wt.% binder with Co:Ni = 85:15, 50:50, and 15:85, together with the present experimental results. In this case, the measured melting temperatures lie close to the calculated melting range. Fig. 7 presents the calculated vertical section of the C-Fe-Ni-W system at 20 wt.% binder with the Fe:Ni = 85:15, 50:50, and 15:85, together with the present experimental results. The experimental values of Lengauer et al. [8] are a little bit higher than the predicted values. Nevertheless, the fit between both data is pretty good.

Fig. 8 demonstrates the vertical sections of C-Co-Fe-Ni-W at 14.3±2 wt.% binder with Fe:Co:Ni = 40:20:40 in comparison with the present experimental results. As it is revealed, the experimental DSC values can be satisfactorily reproduced by the present calculation. Particularly, in the case of Fe+Co+Ni = 12.3 and 13.3 wt% in which the melting onset of the experimental data fits very well with the calculation. Besides, with a binder content of 12.3, 13.3 and 14.3 wt.% the C-window prediction is quite similar to the experimental C-window.

Fig. 9 shows, using the new thermodynamic description, the vertical sections of C-Co-Fe-Ni-W at 20 wt.% binder with Fe:Co:Ni = 62:20:18, 54:20:26, 40:20:40, 51:40:9 and 30:40:30 together with the experimental results of Lengauer et al. [8]. The measured melting temperatures lie close to the calculated melting range. Besides, Table 7 provides a comparison between the Lengauer`s data and this new thermodynamic description. It can be seen the good correlation between both. Work is in progress to analyze the C-window and melting temperatures of quinary systems C-Co-Fe-Ni-W with different Fe:Ni:Co ratios and different binder contents. It is expected to obtain reliable calculations using this new thermodynamic description.

## 6. Conclusions

The phase transformation temperatures of three and four-phase equilibria, i.e., L + fcc + WC , L + fcc + WC + $M_6C$ and L + fcc + WC + C, of WC-14.3 ± 2 wt.% Fe+Co+Ni hardmetals with a ratio of Fe:Co:Ni = 40:20:40 were measured. Also, the C-window was defined accurately with a binder content of 12.3, 13.3 and 14.3 wt.%. A thermodynamic modelling of the C-Co-Fe-Ni-W quinary system was conducted based on the present experimental results and literature data. To verify the rationality of this new database some thermodynamic calculations was carried out. Comparisons between experimental data and theoretical prediction show a good correlation between both. The combination of these experimental results with the thermodynamic predictions could provide an insight on the sinterability this system which is a challenge to the hardmetal industry.

**References**

1. P. Alves, D. Blagoeva, C. Pavel, N. Arvanitidis, Cobalt: demand-supply balances in the transition to electric mobility, JRC Science for policy report, European Commission, 2018. https://ec.europa.eu/jrc/en/publication/eur-scientific-and-technical-research-reports/cobalt-demand-supply-balances-transition-electric-mobility. Date of access: June 28th 2021.

2. L. Prakash, A review of the properties of tungsten carbide hardmetals with alternative binder systems. In: Bildstein H, Eck R, editors. Proc., 13th Plansee Seminar, Reutte, Vol.2; 1993. p. 110–20.

3. L. Prakash, B. Gries, WC hardmetals with iron based binders. In: L. Sigl, P. Rödhammer, H. Wildner, editors. Proc., 17th Plansee Seminar, Reutte, Vol. 2; 2009. HM 5/1.

4. W.D. Schubert, M. Fugger, B. Wittmann, R. Useldinger, Aspects of sintering of cemented carbides with Fe-based binders, Int. J. Refract. Met. Hard Mater. 49 (2015) 110‑123.

5. J. Garcia, V. Collado Ciprés, A. Blomqvist, B. Kaplan, Cemented carbide microstructures: a review, Int. J. Refract. Met. Hard Mater. 80 (2019) 40‑68.

6. A.F. Guillermet, The Co–Fe–Ni–W–C phase diagram: a thermodynamic description and calculated sections for (Co–Fe–Ni) bonded cemented WC tools, Z. Metallkd. 80 (2) (1989) 83–94.

7. B. Uhrenius, H. Pastor, E. Pauty, On the composition of Fe–Ni–Co–WC-based cemented carbides, Int. J. Refract. Met. Hard Mater. 15 (1997) 139–149.

8. P. Zhou, Y. Peng, C. Buchegger, Y. Du, W. Lengauer, Experimental investigation and thermodynamic assessment of the C–Co–Fe–Ni–W system, Int. J. Refract. Met. Hard Mater. 54 (2016) 60–69.

9. T. Soria-Biurrun, L. Lozada-Cabezas, F. Ibarreta-Lopez, R. Martinez-Pampliega, J.M. Sanchez-Moreno, Effect of chromium and carbon contents on the sintering of WC-Fe-Ni-Co-Cr multicomponent alloys, Int. J. Refract. Met. Hard Mater. 92 (2020) 105317.

10. A.T. Dinsdale, SGTE data for pure elements, Calphad 15 (4) (1991) 317–425.

11. Y.M. Muggianu, M. Gambino, J.P. Bros, Enthalpies of formation of liquid alloys bismuth–gallium–tin at 723 K, J. Chim. Phys. Phys. Chim. Biol. 72 (1975) 83–88.

12. M. Hillert, L.I. Staffansson, The regular solution model for stoichiometric phases and ionic melts, Acta Chem. Scand. 24 (1970) 3618–3626.

13. A.F. Guillermet, Thermodynamic analysis of the Co–C System, Z. Metallkd./Mater.Res. Adv. Technol. 78 (10) (1987) 700–709.

14. P. Gustafson, A thermodynamic evaluation of the Fe–C system, Scand. J. Metall. 14 (5) (1985) 259–267.

15. B.J. Lee, On the stability of Cr carbides, Calphad 16 (2) (1992) 121–149.

16. S. Jonsson, "Phase Relations in Quaternary Hard Materials."Ph.D. dissertation, Royal Institute of Technology, Stockholm Sweden, 1993.

17. A.F. Guillermet, Critical evaluation of the thermodynamic properties of the iron–cobalt system, High Temp.–High Pressures 19 (1987) 477–499.

18. A.F. Guillermet, Assessment of the thermodynamic properties of the Ni–Co System,Z. Metallkd. 78 (9) (1987) 639–647.

19. A. Markström, K. Frisk, B. Sundman, A revised thermodynamic description of the Co–W–C system, J. Phase Equilib. Diffus. 26 (2) (2005) 152–160.

20. Zhong Shu Xing, D. D. Gohil, A. T. Dinsdale and T. Chart, National Physical Laboratory, DMA (A) 103, London 1985.

21. P. Gustafson, A thermodynamic evaluation of the C–Fe–W system, Metall. Trans. A 18 (2) (1987) 175–188.

22. P. Gustafson, A. Gabriel and I. Ansara, A Thermodynamic Evaluation of the C-Ni-W System, Z. Metallkde. 78 (1986) 151-156.

23. A.F. Guillermet, Thermodynamic properties of the Fe–Co–C system, Z. Metallkd. 79 (5) (1988) 317–329.

24. A.F. Guillermet, Thermodynamic properties of the Fe–Co–Ni–C system, Z. Metallkd. 79 (8) (1988) 524–536.

25. A. Gabriel, P. Gustafson, I. Ansara, A thermodynamic evaluation of the C–Fe–Ni system, Calphad 11 (3) (1987) 203–218.

26. P. Gustafson, A thermodynamic evaluation of the C–Fe–W system, Metall. Trans. A 18 (2) (1987) 175–188.

27. A.F. Guillermet, Thermodynamic calculation of the Fe–Co–W phase diagram, Z.Metallkd. 79 (10) (1988) 633–642.

28. A.F. Guillermet, L. Ostlund, Experimental and theoretical study of the phase equilibria in the Fe–Ni–W System, Metall. Trans. A 17 (10) (1986) 1809–1823.

29. A.F. Guillermet, Assessment of the Fe–Ni–W–C phase diagram, Z. Metallkd./Mater.Res. Adv. Technol. 78 (3) (1987) 165–171.

30. L. Prakash, Development of Tungsten Carbide Hardmetals Using Iron Based Binder Alloys, PhD Thesis University of Karlsruhe, Germany, 1979.

**Figure captions**

**Fig. 1** BSE-SEM micrographs corresponding to WC-FeNiCo alloys.

**Fig. 2** DSC plots corresponding to WC-FeNiCo alloys.

**Fig. 3** Calculated vertical section of the C-Co-W at 14.3 wt.% binder (red dashed lines) and C-Fe-Co-Ni-W system at 14.3 wt.% binder with Fe:Co:Ni = 40:20:40 (blue solid lines).

**Fig. 4** Calculated vertical section of the (a) C-Co-W system, (b) C-Fe-W and (c) C-Ni-W at 20 wt.% binder, in comparison with Lengauer`s experimental results [8] (the red square symbol corresponds to Lengauer`s alloy with eta phase and the red star symbol corresponds to Lengauer`s alloy with free C).

**Fig. 5** Calculated vertical section of the C-Co-Fe-W system at 20 wt.% binder with Fe:Co = (a) 85:15, (b) 50:50 and (c) 15:85 in comparison with Lengauer`s experimental results [8] (the red square symbol corresponds to Lengauer`s alloy with eta phase and the red star symbol corresponds to Lengauer`s alloy with free C).

**Fig. 6** Calculated vertical section of the C-Co-Ni-W system at 20 wt.% binder with Co:Ni = (a) 85:15, (b) 50:50 and (c) 15:85 in comparison with Lengauer`s experimental results [8] (the red square symbol corresponds to Lengauer`s alloy with eta phase and the red star symbol corresponds to Lengauer`s alloy with free C).

**Fig. 7** Calculated vertical section of the C-Fe-Ni-W system at 20 wt.% binder with Fe:Ni = (a) 85:15, (b) 50:50 and (c) 15:85 in comparison with Lengauer`s experimental results [8] (the red square symbol corresponds to Lengauer`s alloy with eta phase and the red star symbol corresponds to Lengauer`s alloy with free C).

**Fig. 8** Calculated vertical section of the C-Fe-Co-Ni-W system at (a) 12.3 wt.%, (b) 13.3 wt.%, (c) 14.3 wt.%, (d) 15.3 wt.% and (e) 16.3 wt.% binder with Fe:Co:Ni = 40:20:40, in comparison with the present experimental results (the blue square symbol corresponds to alloy 1 with eta phase, the blue triangle symbol corresponds to alloys 2 and 3 within the C window and the blue star symbol corresponds to alloy 4 with free C).

**Fig. 9** Calculated vertical section of the C-Fe-Co-Ni-W system at 20 wt.% binder with Fe:Co:Ni = (a) 62:20:18, (b) 54:20:26, (c) 40:20:40, (d) 51:40:9 and (e) 30:40:30 in comparison with Lengauer`s experimental results [8] (the red square symbol corresponds to Lengauer`s alloy with eta phase and the red star symbol corresponds to Lengauer`s alloy with free C).

Table 1

**Table 1.** Composition of selected WC-Fe-Ni-Co alloys (wt%). All binder phases are based on the same Fe/Ni/Co ratio (in wt%): 40/40/20.

| Ref. | C | W | Fe | Ni | Co |
|---|---|---|---|---|---|
| **Alloy 1** | 5.25 | 80.42 | 5.73 | 5.73 | 2.87 |
| **Alloy 2** | 5.30 | 80.38 | 5.73 | 5.73 | 2.86 |
| **Alloy 3** | 5.34 | 80.35 | 5.73 | 5.72 | 2.86 |
| **Alloy 4** | 5.53 | 80.19 | 5.71 | 5.71 | 2.86 |

Table 2

**Table 2.** Temperatures corresponding to the measured melting onset and the C content of WC-FeNiCo alloys from the present work.

| Ref. | Temperatures of DSC (°C) | C content** (wt.%) |
|---|---|---|
| | Melting onset* | |
| Alloy 1 | 1366 | 5.24 ± 0.01 |
| Alloy 2 | 1360 | 5.28 ± 0.01 |
| Alloy 3 | 1344 | 5.31 ± 0.04 |
| Alloy 4 | 1263 | 5.36 ± 0.03 |

* Data obtained from the heating ramp

**Obtained by infrared spectrometry

Table 3

**Table 3.** Melting temperatures of alloys studied by DSC in comparison with calculated results.

| Four-phase transformation | Experimental data (°C) | Thermodynamic prediction (°C) Present work | Lengauer et al. prediction* (°C) | Lengauer et al. experimental data* (°C) |
|---|---|---|---|---|
| L+fcc+WC+M$_6$C | 1366 | 1366 | 1373 | 1372 |
| L+fcc+WC+C | 1263 | 1262 | 1275 | 1278 |

*As defined in ref. [8]

Table 4

Click here to access/download;Table;Table 4.docx ⬇

**Table 4.** C-window and melting onset predictions, using different databases, of W-C-Fe-Ni-Co system with Fe/Ni/Co ratio (in wt%): 40/40/20 and different binder contents.

| Ref. | Databases | | | | | | | |
|---|---|---|---|---|---|---|---|---|
| | TCFE10 | | Guillermet database* | | Lengauer database** | | Our database | |
| | C-window (wt.%) | Melting onset (°C) | C-window (wt.%) | Melting onset (°C) | C-window (wt.%) | Melting onset (°C) | C-window (wt. %) | Melting onset (°C) |
| **Fe:Co:Ni = 40:20:40 10 wt.% binder** | 5.47-5.56 ($\Delta$C = 0.09) | 1314-1282 ($M_6$C-Free C) | 5.42-5.56 ($\Delta$C = 0.14) | 1282-1229 ($M_6$C-Free C) | 5.49-5.57 ($\Delta$C = 0.08) | 1373-1275 ($M_6$C-Free C) | 5.49-5.57 ($\Delta$C = 0.08) | 1366-1262 ($M_6$C-Free C) |
| **Fe:Co:Ni = 40:20:40 11.8 wt.% binder** | 5.36-5.46 ($\Delta$C = 0.10) | 1314-1282 ($M_6$C-Free C) | 5.29-5.46 ($\Delta$C = 0.17) | 1282-1229 ($M_6$C-Free C) | 5.38-5.47 ($\Delta$C = 0.09) | 1373-1275 ($M_6$C-Free C) | 5.38-5.47 ($\Delta$C = 0.09) | 1366-1262 ($M_6$C-Free C) |
| **Fe:Co:Ni = 40:20:40 12.3 wt.% binder** | 5.32-5.43 ($\Delta$C = 0.11) | 1314-1282 ($M_6$C-Free C) | 5.25-5.43 ($\Delta$C = 0.18) | 1282-1229 ($M_6$C-Free C) | 5.34-5.44 ($\Delta$C = 0.10) | 1373-1275 ($M_6$C-Free C) | 5.34-5.44 ($\Delta$C = 0.10) | 1366-1262 ($M_6$C-Free C) |
| **Fe:Co:Ni = 40:20:40 13.3 wt.% binder** | 5.26-5.38 ($\Delta$C = 0.12) | 1314-1282 ($M_6$C-Free C) | 5.18-5.38 ($\Delta$C = 0.20) | 1282-1229 ($M_6$C-Free C) | 5.28-5.38 ($\Delta$C = 0.10) | 1373-1275 ($M_6$C-Free C) | 5.28-5.38 ($\Delta$C = 0.10) | 1366-1262 ($M_6$C-Free C) |
| **Fe:Co:Ni = 40:20:40 14.3 wt.% binder** | 5.19-5.32 ($\Delta$C = 0.13) | 1314-1282 ($M_6$C-Free C) | 5.11-5.32 ($\Delta$C = 0.21) | 1282-1229 ($M_6$C-Free C) | 5.22-5.32 ($\Delta$C = 0.10) | 1373-1275 ($M_6$C-Free C) | 5.22-5.32 ($\Delta$C = 0.10) | 1366-1262 (M6C-Free C) |
| **Fe:Co:Ni = 40:20:40 15.3 wt.% binder** | 5.13-5.26 ($\Delta$C = 0.13) | 1314-1282 ($M_6$C-Free C) | 5.03-5.26 ($\Delta$C = 0.23) | 1282-1229 ($M_6$C-Free C) | 5.15-5.27 ($\Delta$C = 0.12) | 1373-1275 ($M_6$C-Free C) | 5.15-5.27 ($\Delta$C = 0.12) | 1366-1262 ($M_6$C-Free C) |
| **Fe:Co:Ni = 40:20:40 16.3 wt.% binder** | 5.06-5.21 ($\Delta$C = 0.15) | 1314-1282 ($M_6$C-Free C) | 4.96-5.21 ($\Delta$C = 0.25) | 1282-1229 (M6C-Free C) | 5.09-5.21 ($\Delta$C = 0.12) | 1373-1275 ($M_6$C-Free C) | 5.09-5.21 ($\Delta$C = 0.12) | 1366-1262 ($M_6$C-Free C) |
| **Fe:Co:Ni = 40:20:40 20 wt.% binder** | 4.82-5.00 ($\Delta$C = 0.18) | 1314-1282 ($M_6$C-Free C) | 4.70-4.99 ($\Delta$C = 0.29) | 1282-1229 ($M_6$C-Free C) | 4.85-5.00 ($\Delta$C = 0.15) | 1373-1275 ($M_6$C-Free C) | 4.85-5.00 ($\Delta$C = 0.15) | 1366-1262 ($M_6$C-Free C) |

*As defined in ref. [6]

** As defined in ref. [8]

**Table 5.** C-window predictions, using different databases, of W-C-Co and W-C-Fe-Ni-Co systems with Fe/Ni/Co ratio (in wt%): 40/40/20 and different binder contents.

| Ref. | Databases | | | |
|---|---|---|---|---|
| | TCFE10 | Guillermet database* | Lengauer database** | Our database |
| | C-window (wt.%) | C-window (wt.%) | C-window (wt.%) | C-window (wt.%) |
| **Co** <br> **10 wt.% binder** | 5.39-5.53 <br> ($\Delta C = 0.14$) | 5.39-5.53 <br> ($\Delta C = 0.14$) | 5.39-5.53 <br> ($\Delta C = 0.14$) | 5.39-5.53 <br> ($\Delta C = 0.14$) |
| **Fe:Co:Ni = 40:20:40** <br> **10 wt.% binder** | 5.47-5.56 <br> ($\Delta C = 0.09$) | 5.42-5.56 <br> ($\Delta C = 0.14$) | 5.49-5.57 <br> ($\Delta C = 0.08$) | 5.49-5.57 <br> ($\Delta C = 0.08$) |
| **Co** <br> **11.8 wt.% binder** | 5.26-5.43 <br> ($\Delta C = 0.17$) | 5.26-5.43 <br> ($\Delta C = 0.17$) | 5.26-5.43 <br> ($\Delta C = 0.17$) | 5.26-5.43 <br> ($\Delta C = 0.17$) |
| **Fe:Co:Ni = 40:20:40** <br> **11.8 wt.% binder** | 5.36-5.46 <br> ($\Delta C = 0.10$) | 5.29-5.46 <br> ($\Delta C = 0.17$) | 5.38-5.47 <br> ($\Delta C = 0.09$) | 5.38-5.47 <br> ($\Delta C = 0.09$) |
| **Co** <br> **12.3 wt.% binder** | 5.22-5.40 <br> ($\Delta C = 0.18$) | 5.22-5.40 <br> ($\Delta C = 0.18$) | 5.22-5.40 <br> ($\Delta C = 0.18$) | 5.22-5.40 <br> ($\Delta C = 0.18$) |
| **Fe:Co:Ni = 40:20:40** <br> **12.3 wt.% binder** | 5.32-5.43 <br> ($\Delta C = 0.11$) | 5.25-5.43 <br> ($\Delta C = 0.18$) | 5.34-5.44 <br> ($\Delta C = 0.10$) | 5.34-5.44 <br> ($\Delta C = 0.10$) |
| **Co** <br> **13.3 wt.% binder** | 5.15-5.34 <br> ($\Delta C = 0.19$) | 5.15-5.34 <br> ($\Delta C = 0.19$) | 5.15-5.34 <br> ($\Delta C = 0.19$) | 5.15-5.34 <br> ($\Delta C = 0.19$) |
| **Fe:Co:Ni = 40:20:40** <br> **13.3 wt.% binder** | 5.26-5.38 <br> ($\Delta C = 0.12$) | 5.18-5.38 <br> ($\Delta C = 0.20$) | 5.28-5.38 <br> ($\Delta C = 0.10$) | 5.28-5.38 <br> ($\Delta C = 0.10$) |
| **Co** <br> **14.3 wt.% binder** | 5.08-5.28 <br> ($\Delta C = 0.20$) | 5.08-5.28 <br> ($\Delta C = 0.20$) | 5.08-5.28 <br> ($\Delta C = 0.20$) | 5.08-5.28 <br> ($\Delta C = 0.20$) |
| **Fe:Co:Ni = 40:20:40** <br> **14.3 wt.% binder** | 5.19-5.32 <br> ($\Delta C = 0.13$) | 5.11-5.32 <br> ($\Delta C = 0.21$) | 5.22-5.32 <br> ($\Delta C = 0.10$) | 5.22-5.32 <br> ($\Delta C = 0.10$) |
| **Co** <br> **15.3 wt.% binder** | 5.00-5.22 <br> ($\Delta C = 0.22$) | 5.00-5.22 <br> ($\Delta C = 0.22$) | 5.00-5.22 <br> ($\Delta C = 0.22$) | 5.00-5.22 <br> ($\Delta C = 0.22$) |
| **Fe:Co:Ni = 40:20:40** <br> **15.3 wt.% binder** | 5.13-5.26 <br> ($\Delta C = 0.13$) | 5.03-5.26 <br> ($\Delta C = 0.23$) | 5.15-5.27 <br> ($\Delta C = 0.12$) | 5.15-5.27 <br> ($\Delta C = 0.12$) |
| **Co** <br> **16.3 wt.% binder** | 4.93-5.16 <br> ($\Delta C = 0.23$) | 4.93-5.16 <br> ($\Delta C = 0.23$) | 4.93-5.16 <br> ($\Delta C = 0.23$) | 4.93-5.16 <br> ($\Delta C = 0.23$) |
| **Fe:Co:Ni = 40:20:40** <br> **16.3 wt.% binder** | 5.06-5.21 <br> ($\Delta C = 0.15$) | 4.96-5.21 <br> ($\Delta C = 0.25$) | 5.09-5.21 <br> ($\Delta C = 0.12$) | 5.09-5.21 <br> ($\Delta C = 0.12$) |
| **Co** <br> **20 wt.% binder** | 4.66-4.94 <br> ($\Delta C = 0.28$) | 4.66-4.94 <br> ($\Delta C = 0.28$) | 4.66-4.94 <br> ($\Delta C = 0.28$) | 4.66-4.94 <br> ($\Delta C = 0.28$) |
| **Fe:Co:Ni = 40:20:40** <br> **20 wt.% binder** | 4.82-5.00 <br> ($\Delta C = 0.18$) | 4.70-4.99 <br> ($\Delta C = 0.29$) | 4.85-5.00 <br> ($\Delta C = 0.15$) | 4.85-5.00 <br> ($\Delta C = 0.15$) |

*As defined in ref. [6]

** As defined in ref. [8]

Table 6

**Table 6.** Melting onset, using Lengauer experimental data [8] and the thermodynamic description in the present work, of ternary and quaternary systems at 20 wt.% binder.

| Ref. | Lengauer et al. [8] | Our database |
|---|---|---|
| | Melting onset experimental data ($^0$C) | Melting onset prediction ($^0$C) |
| W-C-Co | 1368-1298 ($M_6$C-Free C) | 1368-1298 ($M_6$C-Free C) |
| W-C-Fe | 1289-1142 ($M_6$C-Free C) | 1265-1139 ($M_6$C-Free C) |
| W-C-Ni | 1434-1335 ($M_6$C-Free C) | 1438-1369 ($M_6$C-Free C) |
| W-C-Co-Fe (Co-Fe = 85:15) | 1353-1277 ($M_6$C-Free C) | 1347-1269 ($M_6$C-Free C) |
| W-C-Co-Fe (Co-Fe = 50:50) | 1321-1223 ($M_6$C-Free C) | 1305-1190 ($M_6$C-Free C) |
| W-C-Co-Fe (Co-Fe = 15:85) | 1298-1163 ($M_6$C-Free C) | 1273-1142 ($M_6$C-Free C) |
| W-C-Co-Ni (Co-Ni = 85:15) | 1378-1304 ($M_6$C-Free C) | 1373-1301 ($M_6$C-Free C) |
| W-C-Co-Ni (Co-Ni = 50:50) | 1403-1319 ($M_6$C-Free C) | 1380-1304 ($M_6$C-Free C) |
| W-C-Co-Ni (Co-Ni = 15:85) | 1425-1329 ($M_6$C-Free C) | 1390-1310 ($M_6$C-Free C) |
| W-C-Fe-Ni (Fe-Ni = 85:15) | 1317-1180 ($M_6$C-Free C) | 1270-1151 ($M_6$C-Free C) |
| W-C-Fe-Ni (Fe-Ni = 50:50) | 1367-1266 ($M_6$C-Free C) | 1317-1236 ($M_6$C-Free C) |
| W-C-Fe-Ni (Fe-Ni = 15:85) | 1414-1330 ($M_6$C-Free C) | 1385-1327 ($M_6$C-Free C) |

Table 7

**Table 7.** C-window prediction and melting onset, using Lengauer data [8] and the thermodynamic description in the present work, of W-C-Fe-Ni-Co system at 20 wt.% binder and different Fe/Co/Ni ratios.

| Ref. | Lengauer et al. [8] | | Our database | |
|---|---|---|---|---|
| | C-window prediction (wt.%) | Melting onset experimental data ($^{o}$C) | C-window prediction (wt.%) | Melting onset prediction ($^{o}$C) |
| Fe:Co:Ni = 62:20:18 20 wt.% binder | 4.99-5.11 ($\Delta C = 0.12$) | 1339-1220 ($M_6C$-Free C) | 4.99-5.11 ($\Delta C = 0.12$) | 1310-1192 ($M_6C$-Free C) |
| Fe:Co:Ni = 54:20:26 20 wt.% binder | 4.94-5.07 ($\Delta C = 0.13$) | 1352-1241 ($M_6C$-Free C) | 4.94-5.07 ($\Delta C = 0.13$) | 1329-1215 ($M_6C$-Free C) |
| Fe:Co:Ni = 40:20:40 20 wt.% binder | 4.85-5.00 ($\Delta C = 0.15$) | 1373-1275 ($M_6C$-Free C) | 4.85-5.00 ($\Delta C = 0.15$) | 1366-1262 ($M_6C$-Free C) |
| Fe:Co:Ni = 51:40:9 20 wt.% binder | 4.96-5.10 ($\Delta C = 0.14$) | 1337-1230 ($M_6C$-Free C) | 4.96-5.10 ($\Delta C = 0.14$) | 1327-1205 ($M_6C$-Free C) |
| Fe:Co:Ni = 30:40:30 20 wt.% binder | 4.86-4.97 ($\Delta C = 0.11$) | 1371-1283 ($M_6C$-Free C) | 4.86-4.97 ($\Delta C = 0.11$) | 1421-1290 ($M_6C$-Free C) |

Support Information

**Experimental and theoretical study of WC-40Fe-20Co-40Ni**

Tomas Soria-Biurrun[1,2] tsoria@ceit.es, Jose M. Sánchez-Moreno[1,2] jmsanchez@ceit.es, Karin Frisk[3,4] friskk@chalmers.se

1- CEIT-Basque Research and Technology Alliance (BRTA), Manuel Lardizabal 15, 20018 Donostia /San Sebastián, Spain.

2- Universidad de Navarra, Tecnun, Manuel Lardizabal 13, 20018 Donostia / San Sebastián, Spain.

3- Chalmers University of Technology, Industrial and Materials Science, SE-412 96 Gothenburg, Sweden.

4- Höganäs AB, SE-263 83 Höganäs, Sweden.

**Table S1.** Summary of the thermodynamic parameters in the C-Co-Fe-Ni-W system[a].

**Liquid:** (C,Co,Fe,Ni,W)$_1$

$$L_{C,Co,Fe}^{liquid} = 11{,}646 - 5.657 * T$$

$$L_{C,Co,Ni}^{liquid} = 50{,}462 - 27.562 * T$$

$$L_{C,Co,W}^{liquid} = (12{,}770 - 22.9 * T)X_C$$

$$L_{C,Fe,Ni}^{liquid} = (122{,}200 - 58.8 * T)X_C + (92{,}200 - 58.8 * T)X_{Fe} + (152{,}200 - 58.8 * T)X_W$$

$$L_{C,Fe,W}^{liquid} = (-60{,}600 - 71 * T)X_C + (6{,}400 - 71 * T)X_{Fe} + (73{,}400 - 71 * T)X_W$$

$$L_{C,Ni,W}^{liquid} = (1100000 - 300 * T)X_C - 235{,}500X_{Ni} + (480{,}000 - 150 * T)X_W$$

$$L_{Co,Fe,W}^{liquid} = 11{,}287X_{Fe}$$

$$L_{Co,Ni,W}^{liquid} = 24{,}655X_{Ni}$$

$$L_{Fe,Ni,W}^{liquid} = 14{,}621X_{Fe} + 64{,}236X_{Ni} - 84{,}842X_W$$

$$L_{C,Co,Ni,W}^{liquid} = 532{,}157$$

$$L_{C,Fe,Ni,W}^{liquid} = -400{,}825$$

**fcc:** (Co,Fe,Ni,W)$_1$(C, Va)$_1$

$$L_{Co,Fe:C}^{fcc} = 313 - 1063\,(y'_{Co} - y'_{Fe})$$

$$L_{Co,Ni:C}^{fcc} = 18{,}289 - 9924\,(y'_{Co} - y'_{Ni})$$

$$L_{Co,W:C}^{fcc} = 87{,}040$$

$$L_{Fe,Ni:C}^{fcc} = 49{,}074 - 7.32 * T - 25{,}800\,(y'_{Fe} - y'_{Ni})$$

$$L_{Fe,W:C}^{fcc} = -116{,}756 + 100 * T$$

$$L_{Fe,Ni,w}^{fcc} = -35{,}044\,y'_{Fe} + 50{,}436y'_{Ni})$$

$$L_{Co,Fe,Ni:C}^{fcc} = -61{,}862$$

**bcc:** (Co,Fe,Ni,W)$_1$(C, Va)$_3$

$$L_{Co,Ni:C}^{bcc} = 6000$$

$$L_{Co,W:C}^{bcc} = -100{,}000$$

$$L_{Fe,Ni:C}^{bcc} = -956.63 - 1.28726 * T + (1789.03 - 1.92912 * T)(y'_{Fe} - y'_{Ni})$$

$$L_{Fe,W:C}^{bcc} = -140{,}000$$

**hcp:** $(Co,Fe,Ni,W)_1(C, Va)_{0.5}$

$$L^{hcp}_{Co,Fe:C} = 8000$$

$$L^{hcp}_{Co,Ni:C} = 6000$$

$$L^{hcp}_{Co,W:C} = 117,000$$

$$L^{hcp}_{Fe,Ni:C} = 49,074 - 7.32 * T - 25,800(y'_{Fe} - y'_{Ni})$$

$$L^{hcp}_{Fe,W:C} = -116,755 + 100 * T$$

$$L^{hcp}_{Ni,W:C} = 2,556 + 11.6 * T - 52,900(y'_{Ni} - y'_{w})$$

**M₆C:** $(Co,Fe,Ni)_2 \; W_2(Co,Fe,Ni,W)_2C_1$

$$G^{M6C}_{Co:W:Co:C} - 4G^{hcp}_{Co} - 2G^{bcc}_{W} - G^{graphite}_{C} = 2,216 - 29.48 * T$$

$$G^{M6C}_{Co:W:W:C} - 2G^{hcp}_{Co} - 4G^{bcc}_{W} - G^{graphite}_{C} = -27,554 - 29.48 * T$$

$$G^{M6C}_{Fe:W:Fe:C} - 4G^{bcc}_{Fe} - 2G^{bcc}_{W} - G^{graphite}_{C} = -63,120 + 20.14 * T$$

$$G^{M6C}_{Fe:W:W:C} - 2G^{bcc}_{Fe} - 4G^{bcc}_{W} - G^{graphite}_{C} = -69,540 + 20.14 * T$$

$$G^{M6C}_{Ni:W:Ni:C} - 4G^{fcc}_{Ni} - 2G^{bcc}_{W} - G^{graphite}_{C} = -8,700 - 4.7 * T$$

$$G^{M6C}_{Ni:W:W:C} - 2G^{fcc}_{Ni} - 4G^{bcc}_{W} - G^{graphite}_{C} = -55,500 - 4.7 * T$$

$$G^{M6C}_{Co:W:Fe:C} - 2G^{hcp}_{Co} - 2G^{bcc}_{W} - 2G^{bcc}_{Fe} - G^{graphite}_{C} = 2,216 - 29.48 * T$$

$$G^{M6C}_{Fe:W:Co:C} - 2G^{bcc}_{Fe} - 2G^{bcc}_{W} - 2G^{hcp}_{Co} - G^{graphite}_{C} = -72,000 + 20 * T$$

$$G^{M6C}_{Co:W:Ni:C} - 2G^{hcp}_{Co} - 2G^{bcc}_{W} - 2G^{fcc}_{Ni} - G^{graphite}_{C} = 2,216 - 29.48 * T$$

$$G^{M6C}_{Ni:W:Co:C} - 2G^{fcc}_{Ni} - 2G^{bcc}_{W} - 2G^{hcp}_{Co} - G^{graphite}_{C} = -8,265 - 29.48 * T$$

$$G^{M6C}_{Fe:W:Ni:C} - 2G^{bcc}_{Fe} - 2G^{bcc}_{W} - 2G^{fcc}_{Ni} - G^{graphite}_{C} = -81,460 + 20 * T$$

$$G^{M6C}_{Ni:W:Fe:C} - 2G^{fcc}_{Ni} - 2G^{bcc}_{W} - 2G^{bcc}_{Fe} - G^{graphite}_{C} = -55,460 + 20 * T$$

$$L^{M6C}_{Fe:W:Fe,W:C} = -43,700$$

**M₁₂C:** $(Co,Ni)_6W_6C_1$

$$G^{M12C}_{Co:W:C} - 6G^{hcp}_{Co} - 6G^{bcc}_{W} - G^{graphite}_{C} = -82,698 - 28.232 * T$$

**Cementite:** $(Co,Fe,Ni,W)_3C_1$

$$G_{Co:C}^{cementite} - 3G_{Co}^{hcp} - G_C^{graphite} = -1567 + 3.963 * T$$

$$G_{Fe:C}^{cementite} = -10{,}745 + 706.04 * T - 120.6 * T \ln(T)$$

$$G_{Ni:C}^{cementite} - 3G_{Ni}^{fcc} - G_C^{graphite} = 34{,}700 - 20 * T$$

$$G_{W:C}^{cementite} - 3G_W^{bcc} - G_C^{graphite} = 54{,}150$$

$$L_{Fe,Ni:C}^{cementite} = 29{,}400$$

**μ:** $(Co,Fe,Ni)_7W_2(Co,Fe,Ni,W)_4$

$$G_{Co:W:Co}^{\mu} - 7G_{Co}^{fcc} - 2G_W^{bcc} - 4G_{Co}^{bcc} = -20{,}534 + 42.774 * T$$

$$G_{Co:W:W}^{\mu} - 7G_{Co}^{fcc} - 2G_W^{bcc} - 4G_W^{bcc} = -26910 - 21.791 * T$$

$$G_{Fe:W:Fe}^{\mu} - 7G_{Fe}^{fcc} - 2G_W^{bcc} - 4G_{Fe}^{bcc} = 0$$

$$G_{Fe:W:W}^{\mu} - 7G_{Fe}^{fcc} - 2G_W^{bcc} - 4G_W^{bcc} = -53{,}450 + 19 * T$$

$$G_{Ni:W:Ni}^{\mu} - 7G_{Ni}^{fcc} - 2G_W^{bcc} - 4G_{Ni}^{bcc} = 1{,}400{,}000$$

$$G_{Ni:W:W}^{\mu} - 7G_{Ni}^{fcc} - 2G_W^{bcc} - 4G_W^{bcc} = 43{,}035$$

$$G_{Co:W:Fe}^{\mu} - 7G_{Co}^{fcc} - 2G_W^{bcc} - 4G_{Fe}^{bcc} = 0$$

$$G_{Fe:W:Co}^{\mu} - 7G_{Fe}^{fcc} - 2G_W^{bcc} - 4G_{Co}^{bcc} = 0$$

$$G_{Fe:W:Ni}^{\mu} - 7G_{Fe}^{fcc} - 2G_W^{bcc} - 4G_{Ni}^{bcc} = 0$$

$$G_{Ni:W:Fe}^{\mu} - 7G_{Ni}^{fcc} - 2G_W^{bcc} - 4G_{Fe}^{bcc} = 0$$

$$G_{Co:W:Ni}^{\mu} - 7G_{Co}^{fcc} - 2G_W^{bcc} - 4G_{Ni}^{bcc} = 0$$

$$G_{Ni:W:Co}^{\mu} - 7G_{Ni}^{fcc} - 2G_W^{bcc} - 4G_{Co}^{bcc} = 0$$

$$L_{Co,Ni:W:W}^{\mu} = -71{,}198$$

---

[a] All parameters are given in J/(mol of atoms); Temperature (T) in K. The Gibbs Energies for the pure elements are taken from the compilation of Dinsdale [10]. The parameters of subbinary systems, which are directly taken from the literature [13-22], and the magnetic contribution to the Gibbs energy for the fcc, bcc and hcp phases from [6], are not listed.